PII: S1350-9462(98)00021-4

Corneal Stromal Wound Healing in Refractive Surgery: the Role of Myofibroblasts

James V. Jester, W. Matthew Petroll and H. Dwight Cavanagh
Department of Ophthalmology, The University of Texas Southwestern Medical Center at Dallas, Dallas, Texas 75235-9057, USA

CONTENTS

Abstract—While laser and incisional refractive surgery offer the promise to correct visual refractive errors permanently and predictably, variability and complications continue to hinder wide-spread acceptance. To explain variations, recent studies have focused on the role of corneal wound healing in modulating refractive outcomes. As our understanding of the corneal response to refractive surgery broadens, it has become apparent that the response of one cell, the corneal stromal keratocyte, plays a pivotal role in defining the results of refractive surgery. Studies reviewed herein demonstrate that injury-induced activation and transformation of keratocytes to myofibroblasts control the deposition and organization of extracellular matrix in corneal wounds. Myofibroblasts establish an interconnected meshwork of cells and extracellular matrix that deposits new matrix and contracts wounds using a novel and unexpected "shoe-string-like" mechanism. Transformation of keratocytes to myofibroblasts is induced in culture by transforming growth factor β (TGFβ) and

Progress in Retinal and Eye Research Vol. 18, No. 3, pp. 311 to 356, 1999

Printed in Great Britain
1350-9462/99/$ - see front matter

blocked *in vivo* by antibodies to TGFβ. Overall, myofibroblast appearance in corneal wounds is associated with wound contraction and regression following incisional keratotomy and the development of "haze" or increased scattered light following laser photorefractive keratectomy (PRK). By contrast, absence of myofibroblasts is associated with continued widening of wound gape and progressive corneal flattening after incisional procedures. Based on these studies, we have arrived at the inescapable conclusion that a better understanding of the cellular and molecular biology of this one cell is required if refractive surgery is ever to achieve predictable and safe refractive results.

1. INTRODUCTION

Heightened interest in refractive surgery over the past 20 years gives testament to the tenacious and pervasive view that corneal curvature and refractive power can be surgically altered predictably and permanently. Attempts to develop, refine, and perfect surgical approaches to the treatment of visual refractive errors has led to the replacement of incisional keratotomy by excimer laser photorefractive keratectomy (PRK) and, more recently, by laser-*in-situ* keratomileusis (LASIK). While the laser has replaced knives, the predictability and permanency of these refractive procedures continue to remain in question. In considering predictability, the foundation of refractive surgery was initially based on the simple model that incision or excision of tissue produces defined changes in corneal curvature. Incisional keratotomy weakens the corneal shell causing an outward bulging and concomitant central corneal flattening (Knauss *et al.*, 1981). By contrast, PRK removes defined amounts of stromal tissue to sculpt the cornea into a defined and predictable surface contour (Puliafito *et al.*, 1987; Trokel, 1989). While explaining the acute effects of surgery, this view has largely ignored any corneal healing response. In fact when first proposed, PRK was thought to result in the formation of a pseudo-basement membrane on which the corneal epithelium migrated and re-attached without further consequence (Fantes *et al.*, 1990). With more extensive research, an awareness of the importance of corneal wound healing in refractive surgery has developed. Variations in the wound healing now appear to not only underlie the varied refractive results and progressive effect of incisional keratotomy (Garana *et al.*, 1992; Jester *et al.*, 1992b; Petroll *et al.*, 1992b) but also determine regression and complications following PRK (Moller-Pedersen *et al.*, 1998a,b). As our understanding of the corneal wound healing response broadens, an expanding body of evidence suggests that the response of one cell, the corneal stromal keratocyte, plays a pivotal role in defining the visual outcome of refractive surgery.

Except for its role in corneal development, the biology of the corneal keratocyte is largely unknown. Structurally and organizationally keratocytes are large, flat cells with long, broad processes that extend and interconnect to adjacent keratocytes through functional gap junctions (Jester *et al.*, 1994; Watsky, 1995). They are interspersed between prominent collagen bundles or lamellae forming from 50 to 100 layers which together comprise the corneal stroma and account for 90% of the corneal thickness (Maurice, 1957, 1962). Corneal keratocytes alone comprise up to 40% of the stromal volume in newborns; decreasing to 10% in the substantially thicker adult cornea (Kaye, 1969). Ultrastructurally, keratocytes contain scant mitochondria and endoplasmic reticulum suggesting quiescence, yet contain stacks of endoplasmic reticulum, large golgi fields, numerous vesicles and fenestrations suggestive of a highly active metabolism (Muller *et al.*, 1995). Functionally, little is known about the keratocyte other than its role in development where it is responsible for synthesizing and organizing the stromal extracellular matrix (Hay, 1980).

While normal corneal keratocytes appear quiescent, injury to the cornea induces a series of phenotypic changes, which ultimately lead to the development of a fibroblastic cell type having ultrastructural, biochemical and physiological properties of myofibroblasts (Luttrull *et al.*, 1985; Jester *et al.*, 1987). Myofibroblasts appear to control the deposition and organization of extracellular matrix in corneal wounds and are responsible for corneal wound contraction. This paper

reviews the evidence establishing the transformation of keratocytes to myofibroblasts and the role of myofibroblasts in corneal stromal wound healing. We propose that it is this transformation process and the subsequent physiological activity of myofibroblasts that ultimately determine the final outcome of refractive surgical procedures. Furthermore, we believe that only through understanding the cellular and molecular mechanisms underlying normal keratocyte function and myofibroblast transformation will we ever be able to achieve predictable and safe refractive surgical results.

2. THE ROAD TO IDENTIFYING THE CORNEAL MYOFIBROBLAST

Wolter (1958) was the first to demonstrate that keratocytes undergo a series of phenotypic changes involving the initial retraction of pseudopodial extensions, elongation to spindle shaped, migratory cells and the later formation of fibroblastic cells in response to corneal wounding. Later electron microscopic studies by Matsuda and Smelser (1973) and Kuwabara *et al.* (1976) documented the ultrastructural changes in the number of mitochondria and the dilation of the endoplasmic reticulum associated with the activation of keratocytes and the commensurate increased biosynthetic activity. Because of the importance of transparency to corneal function, most studies have understandably focused on the biochemical composition, spatial organization and size of the newly synthesized tissue in an attempt to explain corneal opacification following injury and repair (Cintron *et al.*, 1973, 1978, 1982). In these studies sparse interest was given to the closure of the wound or whether corneal wounds contract similar to that which occurs in the skin and other vascularized tissues.

In the skin, the closure and contraction of incisional and excisional wounds has received considerable attention because of the consequent scar constriction leading to significant impairment of tissue and organ function. Abercrombie *et al.* (1956, 1960) were the first to show that dermal wound contraction involved the development of tension within the wound bed or granulation tissue that acted to "pull-in" the wound margins, suggesting that wound healing fibroblasts had structural and functional characteristics similar to smooth muscle. Later studies by Gabbiani *et al.* (1971, 1972) and others (Majno *et al.*, 1971) were the first to discover ultrastructural and physiological similarities between wound tissue fibroblasts and smooth muscle cells. Electron microscopic studies showed that fibroblasts within the wound contained prominent intracellular microfilament (actin) bundles with electron dense bodies similar to that observed in muscle elements of smooth muscle cells (Gabbiani *et al.*, 1971, 1972). Fibroblasts within the wounds also bound antibodies that cross-reacted with smooth muscle cells. Later studies showed that this cross-reactivity was associated with the expression of a vascular smooth muscle specific isoform of actin, α-actin (α-SMA) (Darby *et al.*, 1990; Desmouliere *et al.*, 1992a). Additionally, granulation tissue when loaded on a microforce transducer under physiologic conditions showed *in vitro* contractile responses to smooth muscle agonists (Majno *et al.*, 1971; Luttrull *et al.*, 1985).

Taken together, the ultrastructural, biochemical and physiological data provided convincing evidence that wound healing fibroblasts assume smooth muscle-like characteristics during the process of wound repair. To distinguish this new muscle-like fibroblast phenotype, Gabbiani and co-workers coined the term "myofibroblast". The appearance of myofibroblasts in wound tissue is now recognized as pervasive. In addition to skin, myofibroblast transformation of liver Ito cells are thought to play an important role in the development of liver cirrhosis (Gressner, 1991). In the eye, the presence of myofibroblasts has been implicated in the induction of traction retinal detachment (Ussmann *et al.*, 1980). Transformation of lens epithelial cells to myofibroblasts may also be involved in the process of post-cataract, lens capsule opacification (Hales *et al.*, 1994). In the kidney, myofibroblast transformation of mesangial cells may be important in the development of glomerulosclerosis (Johnson *et al.*, 1992).

While the exact role of myofibroblasts in these and many other pathologic processes remain to be precisely elucidated, it is clear that a diverse

array of cells from different embyological origins have the propensity to acquire similar phenotypic characteristic in response to injury. In the cornea, the first indication that the keratocyte developed these characteristics was suggested by the early studies of incisional wound healing following refractive surgery.

2.1. Incisional Wound Healing in Non-Human and Human-Related Primate Eyes

Incisional keratotomy as first introduced by Fyodorov and Durnev (1979) was a modification of an earlier procedure by Sato *et al.* (1953) which placed both anterior and posterior (endothelial side) incisional wounds in the peripheral

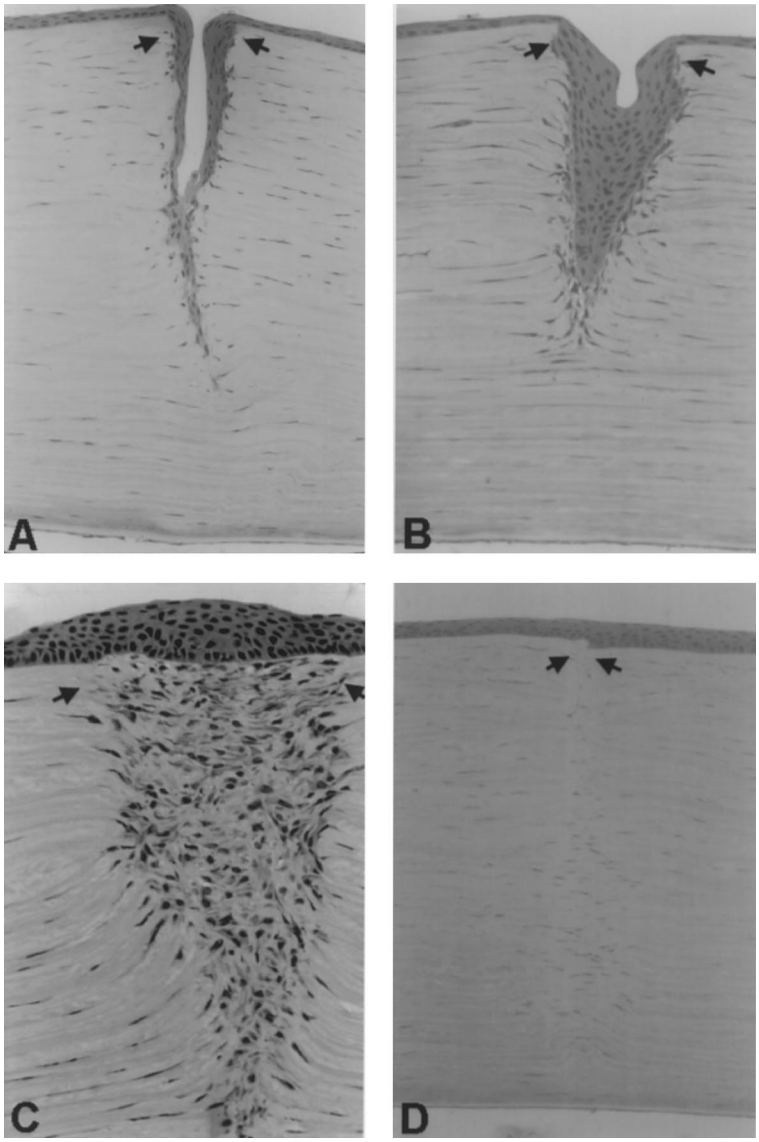

Fig. 1. Histopathology of corneal wounds in owl monkey eyes following partial thickness incisional keratotomy at 3 days (A), 7 days (B), 14 days (C) and 3 months (D). Arrows indicate wound margins. Sections were stained with hematoxylin and eosin. (Original magnification, ×230—A, B, and D; ×270 C).

cornea. Because posterior placement of incisional wounds severely damaged the corneal endothelium, many of the patients receiving the earlier procedure went on to develop bullous keratopathy (Tanaka *et al*., 1980). Although the procedure developed by Fyodorov and Durnev only partially incised the anterior cornea, concern was initially focused on potential damage to the corneal endothelium. Early studies in non-human primates identified a small (~10%) but signficant loss of corneal endothelium (Jester *et al*., 1981; Yamaguchi *et al*., 1984), and later studies have shown this loss not to be progressive or vision threatening.

By contrast, studies of the stromal wound healing response following incisional keratotomy in non-human primate eyes were considered at the time to be consistent with previous observations of corneal wound repair in various animal models. In general, healing of incisional wounds was associated with an early sliding of the corneal epithelium over the wound margins (Fig. 1A) followed by the formation of an epithelial plug (Fig. 1B) that was replaced by proliferating fibroblastic cells (Fig. 1C) leading ultimately to the formation of a linear scar (Fig. 1D). By transmission electron microscopy healing wounds showed the presence of fibroblastic cells containing increased amount of dilated endoplasmic reticulum and the deposition of new connective tissue matrix within the wound margins.

Although these findings reproduced earlier conventional results, clinical and histopathologic correlation between the wound healing response and the refractive effect of incisional keratotomy suggested an important relationship existed between wound gape and refractive effect (Jester *et al*., 1981). By measuring the diopteric power of the central cornea in owl monkey eyes, incisional keratotomy was shown to produce a marked flattening of the central corneal curvature which averaged 4 diopters and 3.25 diopters one month after surgery using 16 and 8 incision keratotomy. This initial flattening effect was followed by a slow regression over six months leaving a residual flattening of only 0.5 diopters and 1.0 diopters in the 16 and 8 incision keratotomized eyes, representing a 4 to 8 fold decrease in refractive effect. This early flattening and later regression of refractive effect was correlated histopathologically with prominent gape of the wound margins at 3, 7 and 14 days after surgery followed by marked reduction of wound gape at 3 months as detected by the separation of Bowman's membrane (Fig. 1A–D, arrows). Measurement of the distance from the cut ends of the original Bowman's membrane and comparison to the original wound gape reaffirmed that significant wound contracture with re-approximation of the wound margins had taken place which correlated with the temporal changes in the refractive effect of incisional keratotomy. It was concluded at that time that the correlation between the loss in corneal flattening and the changes in wound gape suggested that corneal wound healing resulted in a tendency for the cornea to return to its original curvature. Flattening following incisional keratotomy was then proposed to be due in part to the opening of the incision and healing with some residual gape between the original edges of the incision resulting from deposition of new collagen. Whether a similar course of events occurred clinically was not known.

Various pathologic tissue specimens have now been examined by light and electron microscopic techniques. One of the first cases involved a biopsy specimen from a patient who had undergone multiple incisional keratotomy procedures (Jester *et al*., 1983). After receiving circumferential incisions that transected radial incisions, the patient developed broad, grayish-white opacities in the superficial stroma along the incision tracts (Fig. 2A). These were most prominent at the intersections between incisions and appeared to encroach into the stroma four to six months after surgery. The biopsy revealed the presence of retained epithelium within the incised cornea and the absence of fibroblast activity or scarring. Additionally, the incision margins appeared lined by epithelium that had formed an underlying basal lamina with hemidesmosomal attachments adjacent to the incised stroma. These findings suggested that in patients with post-surgical complications that healing of incisional wounds may be delayed, incomplete or absent.

Since this report, penetrating keratoplasty specimens from failed incisional keratotomy and occasional donor tissue has revealed substantial

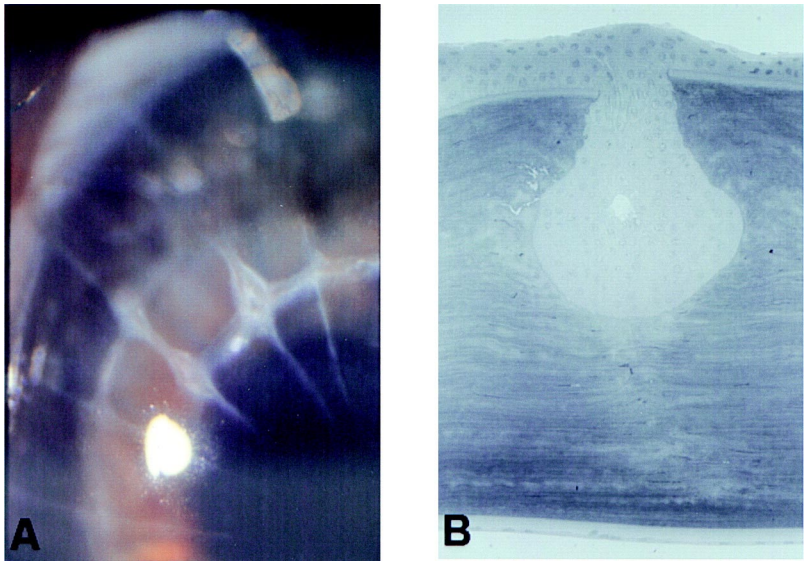

Fig. 2. (A) Patient who received 16 incision keratotomy with two circumferential incisions. Incisions are marked by the presence of grayish-white opacities that appear to encroach into the stroma at the intersections of incisions. (B) Light micrograph of radial incision in a case 26 months after surgery. Present within the radial incision is a prominent epithelial plug that extends halfway into the corneal stroma. (Original magnification, ×100). Taken from Jester *et al.* (1992c, 1983) with permission.

variation in the wound healing response of patients following incisional keratotomy (Deg *et al.*, 1985; Binder *et al.*, 1987; Glasgow *et al.*, 1988; Jester *et al.*, 1992c). Some incisions show wound healing responses similar to that identified in non-human primate eyes with wound closure and fibrosis appearing 6 months to one year after surgery. Many cases, however, show the persistence of epithelial plugs, which can be remarkable years after surgery (Fig. 2B). In general, healing of incisional keratotomy appears to extend over many years with considerable variation in healing rates between individuals, ranging from hypertrophic scar formation to persistent non-healing. Such variations appear to form a clinical spectrum ranging from incomplete healing with persistent wound gape producing gradually increasing refractive over-correction (hyperopic shift) to hypertrophic scar formation with irregular astigmatism and loss of refractive effect. While these cases may represent pathologic extremes, the conclusion that the disparity in the wound healing patterns of patients underlies the exceedingly wide predictability of incisional refractive results is inescapable. Furthermore, since the disparity of wound healing patterns determines, for the most part, the amount of residual wound gape, understanding what cellular and molecular mechanisms control wound gape is clearly critical to understanding the effects and predictability of incisional refractive surgery.

2.2. Characterization of Wound Healing Fibroblasts

As mentioned above, closure of skin wounds was shown by Gabbiani *et al.* (1971) to involve the transformation of dermal fibroblasts to a myofibroblast phenotype. However, a similar cell type with muscle-like characteristics had not been identified in the cornea prior to the development of incisional keratotomy. In fact, early attempts to identify myofibroblasts in healing corneal wounds had been negative (Schachar *et al.*, 1980; Jester *et al.*, 1981). Furthermore, since wounds in skin were associated with neovascularization and since myofibroblasts developed vascular smooth muscle-like characteristics with the expression of smooth muscle actin, it was not clear in the early 1980's whether avascular corneal wounds healed by a similar mechanism. In order to address this question a detailed study of the morphological,

biochemical and physiological characteristic of wound healing fibroblasts was undertaken.

2.2.1. *Morphological and biochemical identification*

Using a rabbit wound healing model previously developed by Cintron *et al.* (1973) in which avascular corneal wounds healed by scar formation, the transformation of keratocytes to wound healing fibroblasts was evaluated (Jester *et al.*, 1987). In this model, full thickness trephination wounds in the central cornea were initially sealed by the formation of a fibrin plug within 4 hours after injury. By seven days a loose connective tissue matrix containing fibroblastic-like cells (Fig. 3A) replaced the fibrin plug. Ultrastructural evaluation of keratocytes adjacent to the wound showed a clear transition from normal quiescent keratocytes to activated keratocytes containing prominent golgi and extensive rough endoplasmic reticulum. Cells within the wound however, showed the development of an extensive microfilament network closely approximated to the plasma membrane within the cortex of the cell. Additionally, accumulations of microfilament networks were detected at the leading edge of cells that were in close association with adjacent cells

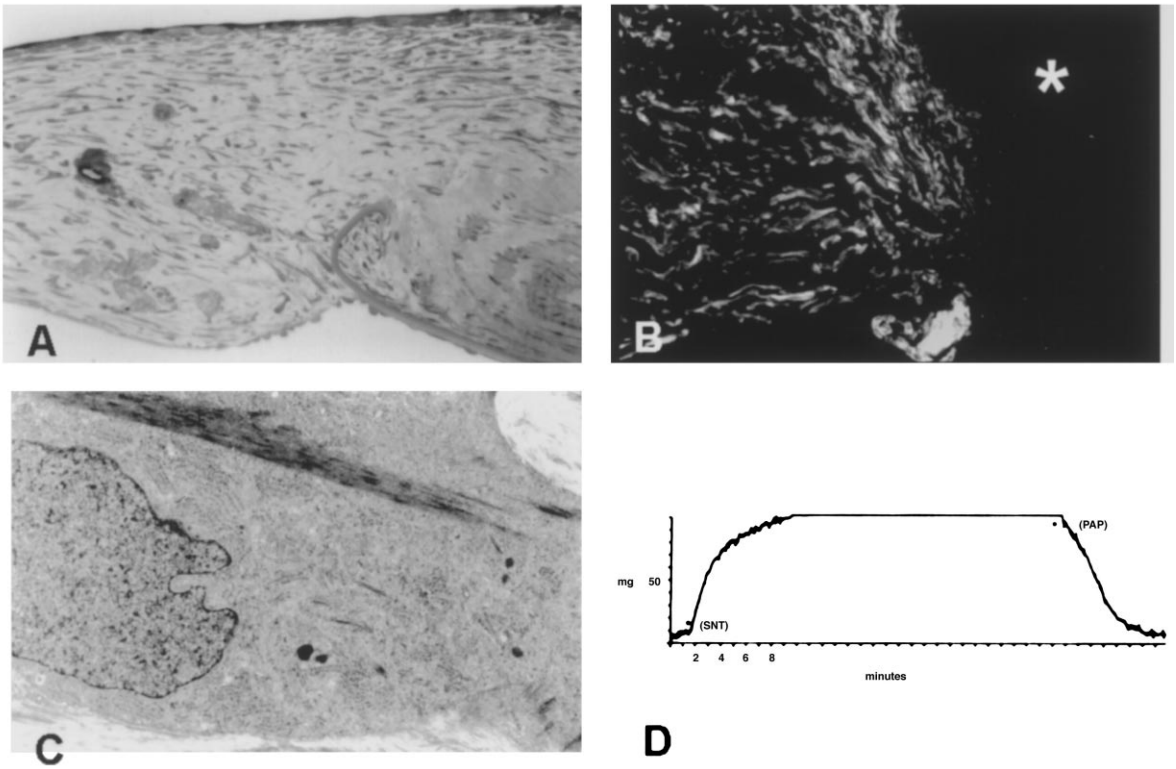

Fig. 3. (A) Central corneal trephination wound in the rabbit eye, 7 days after injury. The wound contains for the most part a loose connective matrix with fibroblast (Toluidine blue, original magnification ×162). (B) Frozen section of 7 day old wound stained with NBD-phallacidin. Note the marked staining of cells within the wound and the migration pattern forming pseudo-lamellar layers. Adjacent to the wound within the corneal stroma (asterisk), NBD-phallacidin fluorescence was barely detectable in normal and activated keratocytes. (Original magnification, ×250). (C) Transmission electron micrograph of corneal wound healing fibroblast 1 month after injury. Note the prominent microfilament bundle containing electron-dense bodies similar to that observed in stress fibers, smooth muscle cells and skin myofibroblasts. (Uranyl acetate and lead citrate, original magnification, ×11 000). (D) Response of avascular corneal wound tissue to serotonin (5-HT). Note the characteristic contraction response curve and over 100 mg of force generated by the specimen. Relaxation was elicited by addition of papaverine (PAP). Asterisk marks time agents were added. Taken from Jester *et al.* (1987) and Luttrull *et al.* (1985) with permission from the Association for Research in Vision and Ophthalmology.

through putative cell–cell junctions. These cell–cell junctions were similar to the cell–cell junctions previously described by Gabbiani *et al.* (1978) for skin myofibroblasts.

Using the fluorescent probe NBD-phallacidin, a derivative of the mushroom toxin, phalloidin, which specifically binds to actin filaments (f-actin) and oligomeres of g-actin, confirmed the increased appearance of microfilaments. Stained frozen sections from wounds at 7 days showed a marked increase in NBD-florescence of fibroblastic cells within the wound compared to adjacent activated and normal keratocytes (Fig. 3B). This staining increased in intensity from 2 weeks to 2 months after injury. On an ultrastructural level, the increased NBD-phallacidin staining was associated with the organization of cortical microfilaments into prominent microfilament bundles and arrays (Fig. 3C). The microfilament bundles also contained electron-dense bodies similar to those observed in smooth muscle cells and skin myofibroblasts. Biochemical characterization of normal corneal tissue and wound tissue also showed grossly similar protein patterns and isoelectric focusing gels detected predominantly the γ-isoform of actin, characteristic of non-muscle cells. Although no α-SMA was detected in this study, contamination of wounds by vascular smooth muscle cells seemed unlikely since such cells would have to migrate from the limbus to the wound through the corneal stroma. Furthermore, in so doing, vascular smooth muscle cells would have to assume a non-muscle-like phenotype similar to keratocytes while in the stroma and then reassume a smooth muscle phenotype once within the wound. Overall, these morphologic and biochemical findings suggested that adjacent corneal keratocytes transformed to a smooth muscle-like, myofibroblast phenotype in response to corneal injury.

2.2.2. *Physiological characteristics*

Since granulation tissue myofibroblasts show contractile behavior when stimulated by smooth muscle agonists, the ability of corneal myofibroblasts to show contractile properties was also evaluated. Rabbit corneal tissue, 3 to 4 weeks after trephination injury, were removed and placed on a microforce transducer under *in vitro*, physiologic conditions. When wound tissue was stimulated with epinephrine, norepinephrine, and serotonin, there developed a characteristic contractile response in which the wound tissue generated up to 100 mg of force (Fig. 3D). No response was detected to acetylcholine, vasopressin or histamine, all of which elicited contractile responses from iris tissue, a possible contaminant of the corneal wounds. Furthermore, no contractile response was detected in tissue from unwounded cornea. Overall, these studies indicated that in addition to the morphologic similarities between corneal wound healing fibroblasts there were clear physiologic and functional similarities strongly implicating corneal myofibroblasts in a wound contractile process.

2.3. Wound Contraction, Corneal Myofibroblasts and Incisional Keratotomy

Although corneal myofibroblasts could be detected in corneal wounds, their relationship to wound contraction and the refractive changes following incisional keratotomy remained unclear. Three basic models had been proposed to explain the refractive effect of incisional keratotomy which included; (1) transsection of the ligament of Kokott (Kokott, 1938; Fyodorov and Durnev, 1979, 1981); (2) global stretching of the anterior cornea (Schachar *et al.*, 1981); and (3) peripheral corneal weakening with concomitant peripheral bulging and central corneal flattening (Knauss *et al.*, 1981). Key to differentiating between these hypotheses was the determination of changes in wound gape and their correlation to the refractive effect. Measurement of wound gape, however, was initially limited to conventional histopathologic observations in which the tissue was excised, fixed, sectioned and stained. Unfortunately, the processing of tissue induced artifacts caused by tissue dehydration and sectioning which made difficult or impossible the direct correlation of any change in wound gape to the refractive results. Furthermore, the variability in individual responses, even in a defined animal model, made it difficult to relate any histopathologic data

obtained from one eye to the clinical data of another.

In 1986, however, Lemp *et al*. (1986) published the first report on the use of a new, optical microscope using confocal theory which provided detailed histopathologic evaluation of the *ex vivo* cornea without the need to excise, fix and section tissue specimens. Since this first report, several confocal microscopes have been developed and used to "optically" section tissue, non-invasively rather than using a tissue microtome. [For a detailed review see Cavanagh *et al*. (1995)]. Using this form of microscopy it was apparent, for the first time, that *in vivo* histopathologic evaluation

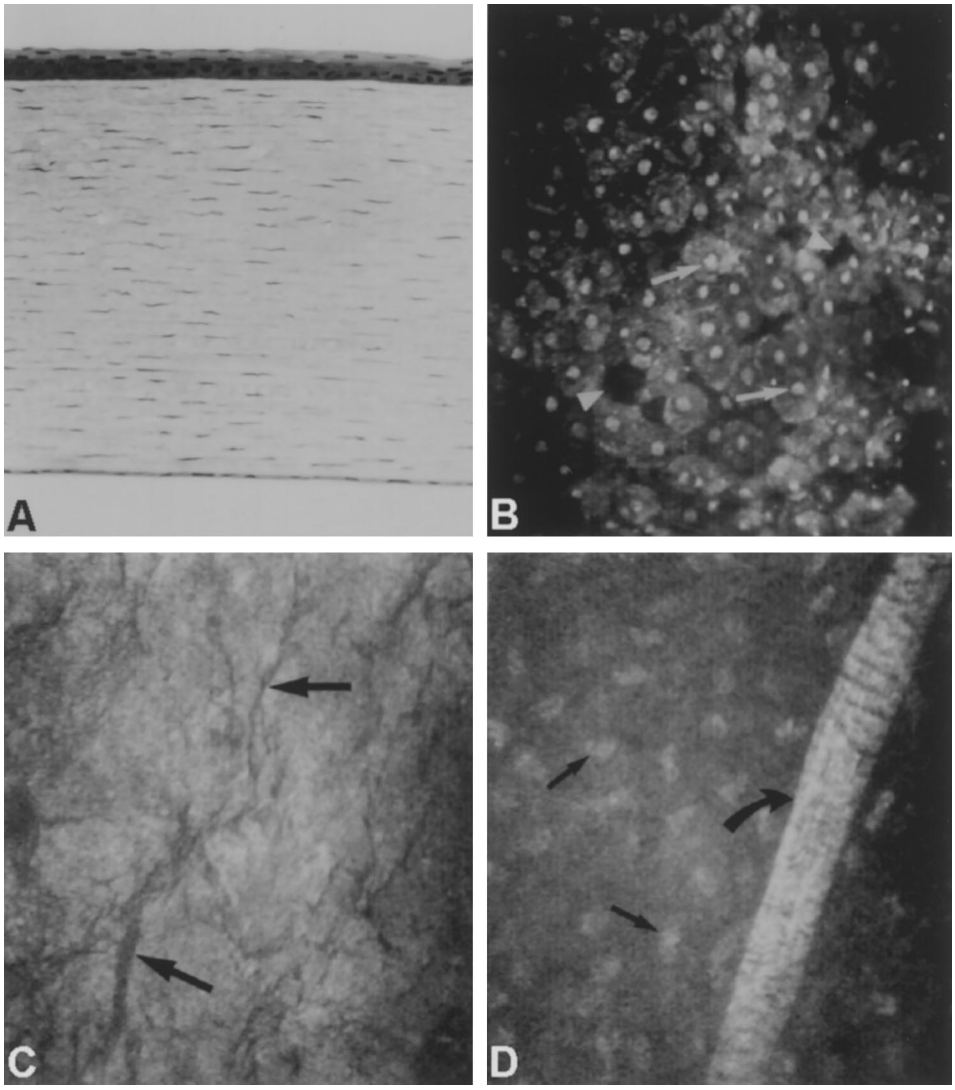

Fig. 4. Comparison of the normal light microscopic image (A) to *in vivo*, confocal microscopic image of the corneal epithelium (B), basal lamina (C), and stroma (D). Note that images from the confocal microscope provide an *en face* orientation to the tissue similar to scanning electron microscopic images. In B, surface epithelial cells appear as broad, flat, overlapping cells with brightly reflecting nuclei (arrows). Dark spaces between some cells (arrowheads) suggest irregularities in the topography of the surface epithelium. In C, the basal lamina shows a variegated appearance with multiple dark lines (arrows). Below the basal lamina in C, images of the corneal stroma show brightly reflecting keratocyte nuclei (arrows) and occasional nerves (curved arrow). (Original magnification: ×240 for A and ×230 for B–D) Taken from Jester *et al*. (1992b) with permission from the Association for Research in Vision and Ophthalmology.

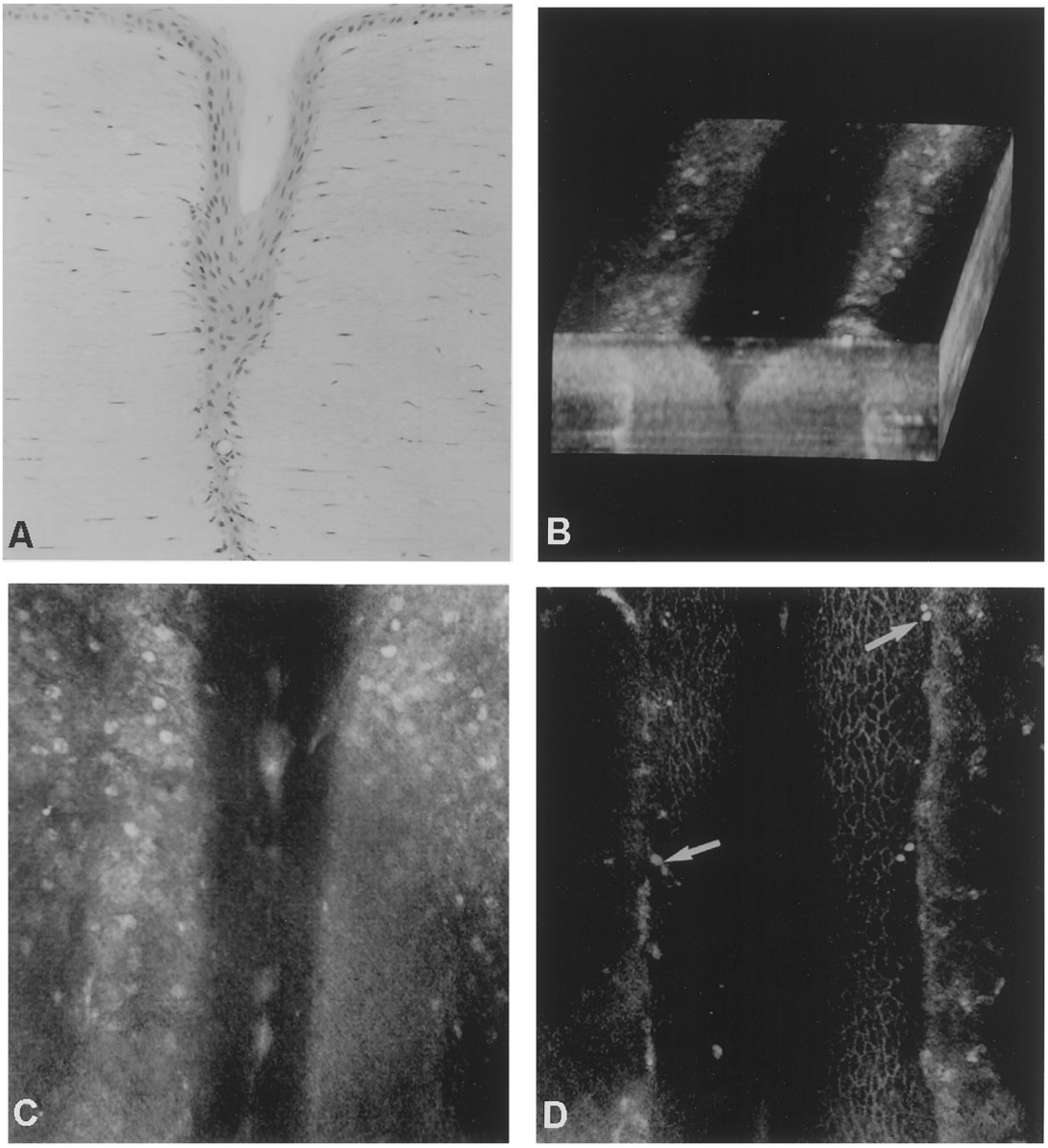

Fig. 5. Histopathologic micrograph (A) of incised cornea 3 days after keratotomy compared to confocal microscopic reconstruction of the wound from a living cat eye (B–D). By 3 days, the surface epithelial sheet has migrated into the corneal incision and lines the cut surfaces of the stroma as seen in cross-section using routine histologic processing (A) and the orthogonal cabinet projection (B). In B, single images that comprise the stack can be paged through to reveal details of the cells surrounding the wound (C and D). At the surface of the wound (C) the epithelium appears to be elevated above that overlying the uncut stroma suggesting localized stromal edema. Deeper into the stroma (D) details of the epithelial cell borders within the epithelial plug can be detected suggesting pooling of fluid around the cells and intercellular edema. Between epithelial cells, bright bi-lobed reflections indicate presence of inter-epithelial and stromal inflammatory cells (arrows). (Original magnification: A, ×178; B, ×190; and C, D, ×260). Taken from Jester *et al.* (1992b) with permission from the Association for Research in Vision and Ophthalmology.

could be made, temporally, over time, in the same living eye, and the results directly correlated to the clinical findings. Using this form of microscopy, detailed study of the changes in wound gape were made in both a cat and non-human primate model of incisional keratotomy and the results correlated with histopathological, immunocytochemical and clinical findings (Garana *et al*., 1992; Jester *et al*., 1992b; Petroll *et al*., 1992b).

2.3.1. *In vivo confocal microscopy of corneal wounds*

In the normal cornea *in vivo* confocal microscopy detected images from corneal structures that prominently reflected light (Fig. 4), including the superficial epithelium (B), basal lamina (C) and the nuclei of corneal keratocytes and nerve bundles (D). Following incisional keratotomy, the optical sectioning abilities of the confocal microscope allowed serial imaging of the corneal

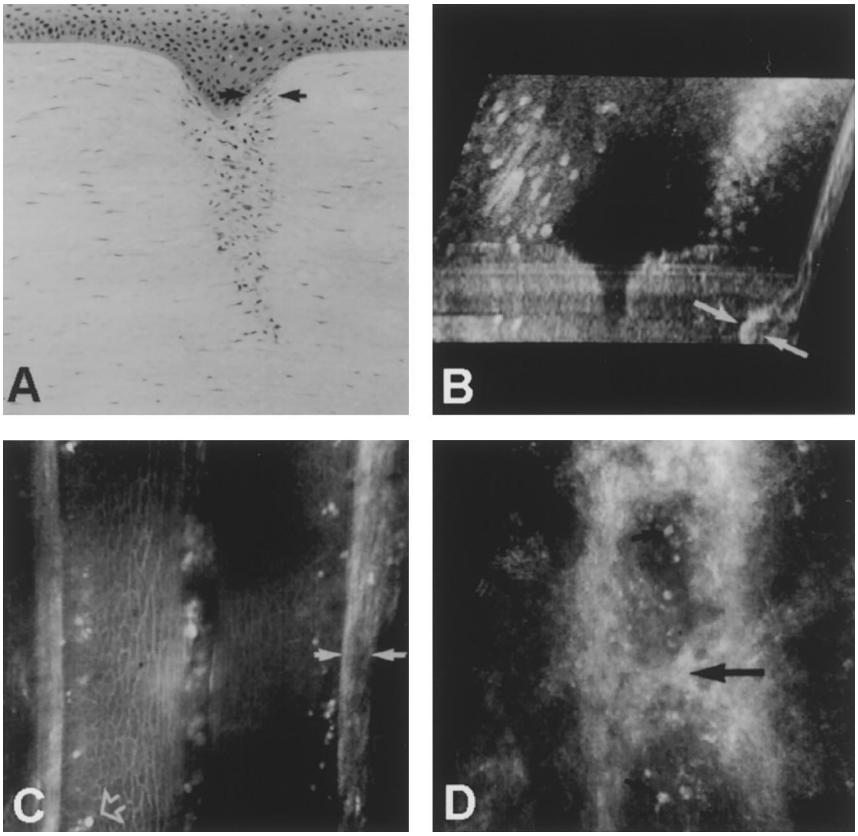

Fig. 6. Histopathologic (A) and *in vivo*, confocal microscopic images (B–D) of incisional keratotomy wounds 14 days after surgery. Confocal images taken of the same wound shown in Figure 5 B–D. Initiation of wound contraction correlated with the in-growth of wound healing fibroblasts between the corneal stroma and the epithelial plug (A, between arrows) which was seen by confocal microscopy as a region of reflective cells lining the wound margin (B, between arrows). In individual optical slices (C) the subepithelial area adjacent to the corneal stroma appeared to be composed of spindle shaped clles (between arrows). Within the epithelial plug, persistence of inflammatory cells was detected (open arrow). At the base of the epithelial plug (D) the highly reflective, spindle shaped cells appeared to become more randomly oriented (large arrow) while inflammatory cells or degenerative epithelial cells were detected within the basal epithelial cells (small arrows). (Original magnification: A, ×178; B, ×190; C, D, ×260). Taken from Jester *et al*. (1992b) with permission from the Association for Research in Vision and Ophthalmology.

wounds along the entire length of the incision, establishing an *in vivo* incision profile. In the cat, the wound gape at the level of Bowman's membrane appeared to vary along the length of the wound from the central to peripheral cornea. At the widest point (approximately 2.4 mm peripheral to the beginning of the incision) the wound gape measured 135 μm in width immediately after surgery. At 3 days, wound gape measured approximately 203 μm, or an increase of 68 μm in width compared to wounds immediately after surgery. Histopathologically, 3-day-old incisional wounds in the cat showed migration of the epithelium into the wound similar to that seen in non-human primate eyes (Fig. 5A). Using confocal microscopy, the living wound was three-dimensionally reconstructed by stacking and manually aligning a series of 2-dimensional images that extended approximately 140 μm into the living tissue. The reconstruction was then rotated to provide a cross-sectional view similar to that obtained by conventional histopathology (Fig. 5B). In the 3-dimensional reconstruction, the epithelial sheet appeared to line separately

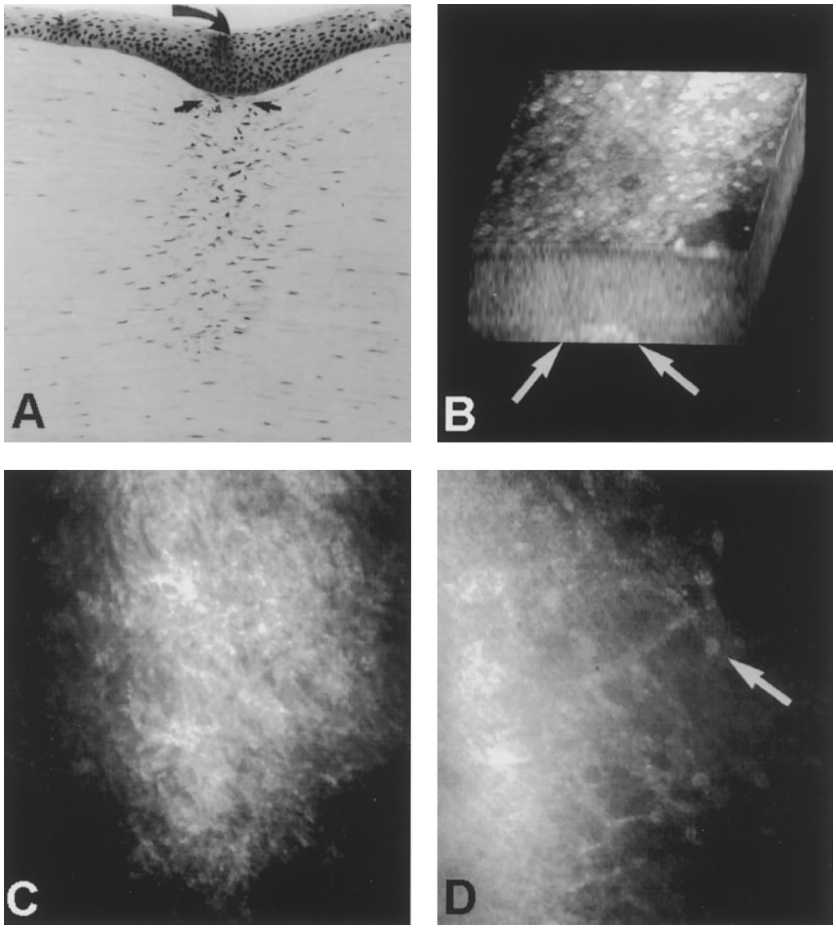

Fig. 7. Histopathologic (A) and confocal microscopic (B–D) images of incisional keratotomy wounds 30 days after surgery. Confocal images were taken of the same incision shown in Fig. 5B–D and Fig. 6B–D. Both the histopathologic (A) and the 3-dimensional confocal images (B) show a marked reduction wound gape (between arrows). In the histopathologic micrograph the epithelial surface appears invaginated (A, curved arrow), a similar invagination was not seen by confocal microscopy (B). In single optical sections (C) the area of wound fibrosis appeared as an irregular network of highly reflective structures representing either extracellular matrix or fibroblasts. Deeper within the wound (D) individual keratocyte cell bodies were seen bordering the wound margin (D, arrow). Taken from Jester *et al.* (1992b) with permission from the Association for Research in Vision and Ophthalmology (Original magnification: A, ×178; B, ×190; C, D, ×260).

both sides of the stromal wound with a space separating the two epithelial layers. Individual images comprising the 3-dimensional stack showed the presence of inflammatory cells (D, arrows) and the beginning activation of keratocytes immediately adjacent to the incision. At this time no keratocytes were detected within the margins of the wound.

From day 3 to day 7, wound gape continued to increase in width to approximately 245 μm at the midperiphery. By day 14, however, wounds showed a reduction in gape to 198 μm. This reduction in wound gape correlated with the replacement of the epithelial plug with wound healing fibroblasts as seen by histopathologic and confocal microscopic examination (Fig. 6A, B, between arrows). Adjacent to the epithelium, wound-healing fibroblasts appeared as spindle-shaped cells aligned parallel to the wound margin (Fig. 6C). However, deeper within the wound the fibroblasts became more irregularly arranged and appeared to become interwoven; extending between and spanning the wound margins (Fig. 6D, arrow). By 30 days after surgery, there was considerable reduction in wound gape to 92 μm in width. This reduction correlated with the complete loss of the epithelial plug and replacement with wound healing fibroblasts (Fig. 7A, B). Single, confocal sections showed the wound area to be comprised of higly reflective structures (Fig. 7C), that were difficult to distinguish. Deeper within the wound, adjacent keratocytes appeared as an interconnected network that appeared oriented toward the wound and possibly interconnected with wound healing fibroblasts (Fig. 7D).

Overall, the confocal measurement of wound gape in the cat demonstrated for the first time a biphasic healing response with wound gape initially increasing till day 10 and decreasing from day 14 to day 30. While edema may explain, in part, the development of wound gape, there is no clear explanation for increasing edema from day 0 to day 10 to explain the increasing wound gape over this time. Rather, these findings suggested that healing of incisional keratotomy was associated with a distinct non-contractile and contractile phase, which depended on the presence, or absence of wound healing fibroblasts.

2.3.2. *The corneal myofibroblast contractile apparatus*

Although corneal wound healing fibroblasts in full thickness wounds appeared to develop characteristics of skin myofibroblasts, it remained to be determined if the fibroblasts detected during the contractile phase of incisional wound healing showed similar characteristics. In order to answer this question, electron microscopy and fluorescent antibody staining to detect the presence and organization of actin and actin binding proteins (Garana *et al.*, 1992) were used to evaluate incisional wounds from cat eyes. As shown for full thickness rabbit corneal wounds, wound-healing fibroblasts from feline partial thickness, incisional wounds showed development of prominent microfilament bundles containing electron dense bodies similar to skin myofibroblasts. Additionally, fibroblasts, which replaced the epithelial, plug at day 14 after surgery showed prominent staining by FITC-conjugated phallacidin (Fig. 8E) which binds specifically to f-actin, confirming the electron microscopic results. Interestingly, activated keratocytes adjacent to the wound at day 3 to day 7 (Fig. 8D) did not stain intensely with phalloidin. These findings indicated that during the non-contractile phase of incisional wound healing, f-actin is predominantly localized to the corneal epithelium. Furthermore, the initiation of the contractile phase at day 14 was associated with a marked increase in the f-actin organization within wound healing fibroblasts, exclusively localized within the wound.

By contrast, fibronectin, which is a prominent extracellular matrix constituent of wound tissue, appeared to be deposited along the wound edge, extending along lamellae, prior to the development of actin filaments within activated keratocytes (Fig. 8A, arrow). Additionally, replacement of the epithelial plug with wound healing fibroblast at the initiation of wound contraction (day 14) was associated with a random organization of fibronectin and f-actin (Fig. 8B, E). By day 30 both the f-actin and fibronectin organization showed a distinct alignment suggestive of a lamellar organization (Fig. 8C, F). Taken together these data suggested that the initiation of wound contraction correlated with formation of randomly organized intracellular f-actin and extra-

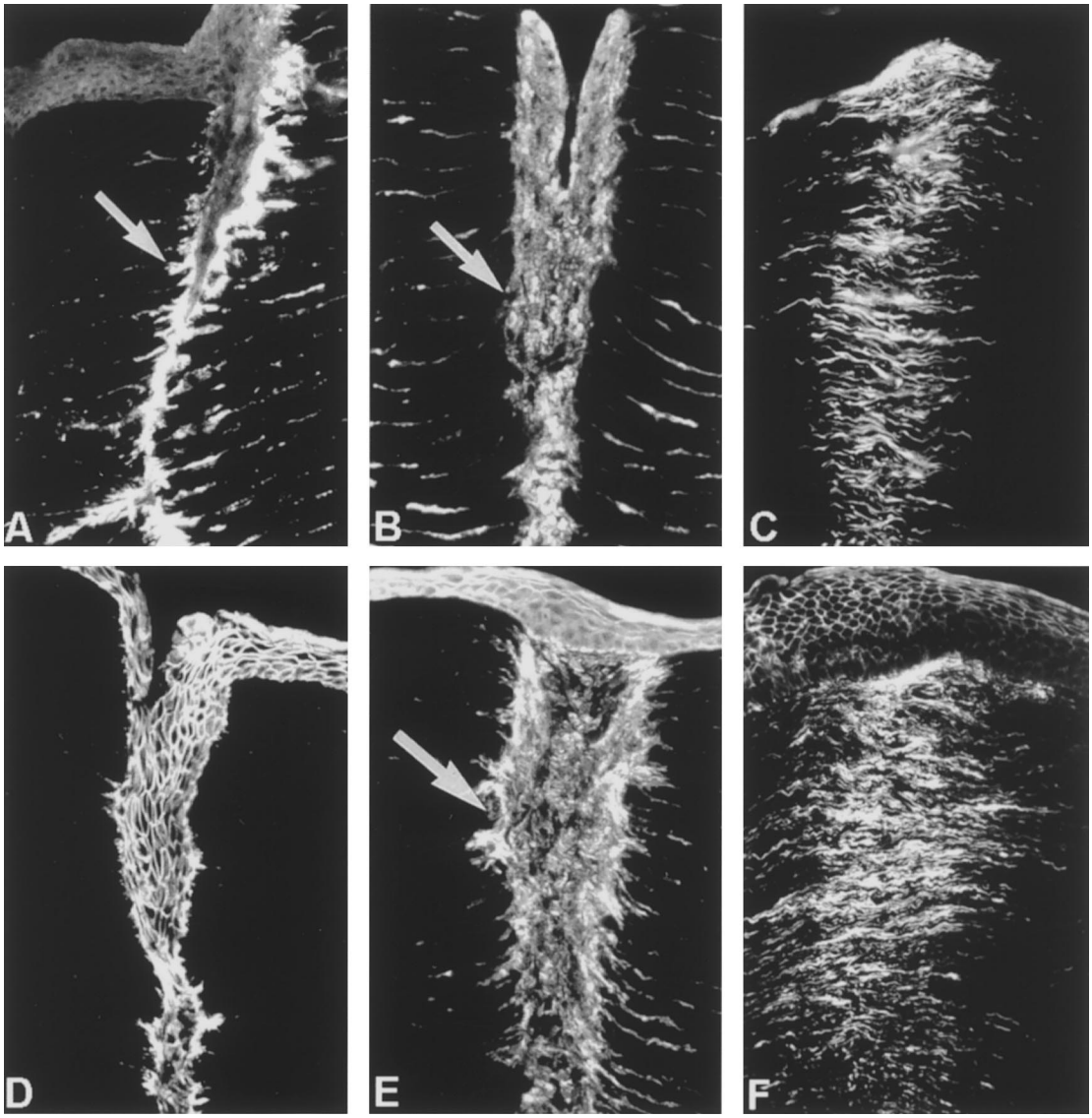

Fig. 8. Cat incisional keratotomy at 3 (A, D), 14 (B, E) and 30 (C, F) days after surgery stained with FITC-conjugated goat anti-human fibronectin (A–C) and FITC conjugated phallacidin (D–F). Three days after surgery, anti-fibronectin antibodies (A) stained the stromal wound edge with staining extending along the stromal lamellae (arrow). At the same time, FITC-phallacidin (D) appeared to stain the cortex of the migrating epithelium but only weakly stained adjacent keratocytes. By day 14, developing fibrotic tissue showed intense staining with both anti-fibronectin (B) and phallacidin (E) (arrows). Additionally keratocytes adjacent to the wound showed increased staining but not as intense as that observed in fibroblasts within the wound. At day 30, anti-fibronectin (C) and phallacidin (F) appeared organized into parallel bundles. (Original magnification, ×200). Taken from Garana *et al.* (1992) with permission from the Association for Research in Vision and Ophthalmology.

cellular fibronectin that became organized along *parallel* lamellar planes during the wound contraction process.

The association between fibronectin and actin was further evaluated in this study by staining of wounds with antibodies against non-muscle myosin, α-actinin, and $\alpha_5\beta_1$ integrin [the high affinity fibronectin receptor (Akiyama *et al.*, 1989)]. The results of these immunolocalization studies indicate that prominent microfilament bundles pre-

sent within wound healing fibroblast contain both non-muscle myosin and α-actinin which combine to form a smooth muscle-like contractile unit similar to stress fibers in cultured fibroblasts. Furthermore, the localization of $\alpha_5\beta_1$ integrin along f-actin bundles indicated that this integral membrane receptor linked intracellular microfilaments to extracellular fibronectin, forming a putative contractile structure. As proposed by Welch *et al.* (1990), the data supported the hypothesis that interactions between extracellular fibronectin and intracellular f-actin, myosin and α-actinin mediated by $\alpha_5\beta_1$ integrin acted together to "pull-in" extracellular matrix to form fibronectin fibrils and exert force leading to wound contraction by a novel and previously unsuspected "shoe-string" tightening mechanisms.

2.3.3. *Temporal changes in wound gape and refractive effect in incisional keratotomy*

In order to determine the final role of wound healing on incisional refractive surgery, changes in wound gape as measured by confocal microscopy were correlated with the changes in keratometry following surgery in non-human primate eyes. As shown for the cat, non-human primate eyes exhibited a biphasic wound contractile response with increasing wound gape detected from day 3 to day 7 and a decreasing wound gape from day 14 to 45 (Fig. 9A). Furthermore, decreasing wound gape was directly associated with development of wound fibrosis and the replacement of the epithelial plug. Concurrent measurement of corneal curvature in the same eyes detected an increasing corneal flattening effect of incisional keratotomy from day 3 to day 7 and a progressive regression of effect from day 14 to day 45 (Fig. 9B). Although there was inter-animal variation, the mean temporal changes in corneal curvature significantly paralleled the changes in wound gape ($r = -0.96$).

Extending the findings of the cat to the primate and primate to human suggested that the disparity in wound healing shown in pathologic cases of incisional keratotomy underlie the variation in refractive outcomes observed clinically. Furthermore, this variation was directly related to the appearance and function of one cell, the myofibroblast. Specifically, in the absence of the myofibroblast (days 0 to 10) there is a slow but progressive increase in incision width leading to ever greater corneal flattening. After the appearance of myofibroblasts (day 14) there is initiation of wound contraction and a re-steeping of the cornea. These findings exactly parallel the clinical findings in that progressive hyperopia seen in 20% of patient following incisional keratotomy (Waring *et al.*, 1994) appears to show delayed wound healing (Jester *et al.*, 1992c). It also predicts that those patient showing a normal wound healing response, wound contraction as mediated by the myofibroblast will tend to reverse the refractive effect explaining regression in these eyes.

3. CORNEAL MYOFIBROBLASTS IN 3 AND 4 DIMENSIONS

Thus far, studies of corneal wound healing following partial and full thickness injury had focused on explaining the refractive effect of incisional keratotomy and had not addressed the basic question of how myofibroblast contract wounds. Structurally, myofibroblasts contained a putative contractile apparatus comprised intracellularly of f-actin, non-muscle myosin and α-actinin, and extracellularly of fibronectin that were potentially linked by the surface membrane receptor, $\alpha_5\beta_1$ integrin. The appearance of myofibroblasts in the wound correlated with wound contraction, or the re-apposition of wound margins, and, under *in vitro* conditions, the development of contractile responses. While these morphological, biochemical and physiological characteristics suggest that myofibroblasts were capable of exerting muscle-like contractile forces within wounds, the exact mechanism has yet to be determined. In order to begin to address this question, we performed 3 and 4-dimensional studies of the corneal myofibroblast to identify the temporal-spatial organization of myofibroblasts within wounds.

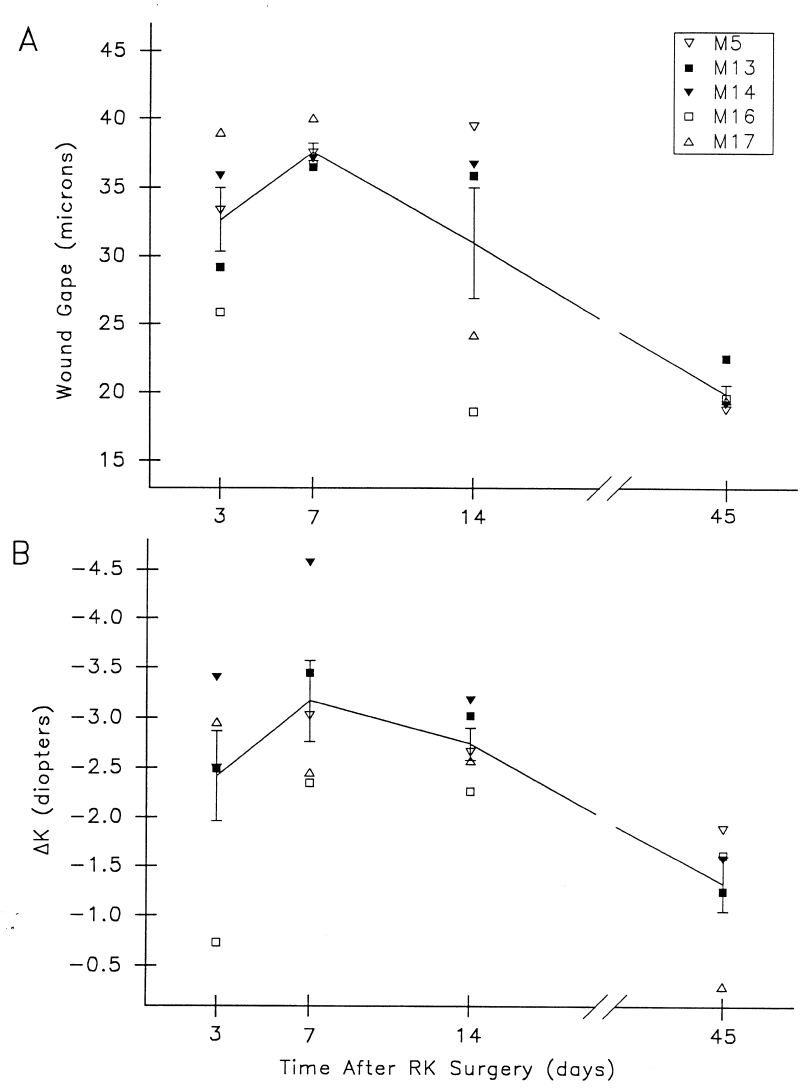

Fig. 9. Temporal changes in (A) wound gape and (B) corneal curvature (K) for individual animals (symbols) and mean data (solid lines) after incisional keratotomy. Error bars represent standard error of the mean ($n = 5$). Taken from Petroll *et al.* (1992b) with permission from the Association for Research Vision and Ophthalmology.

3.1. Alignment of Contractile Structures During Healing

Since the microfilament bundles within myofibroblasts were thought to exert force within wounds, in a contractile model, the forces generated by f-actin would be directed along the axis of the microfilament bundle. Characterization of the changes in the 3-dimensional, spatial and temporal organization during healing would therefore provide insights into the mechanism of wound contraction and highlight the role of the putative contractile apparatus. In order to study these organizational changes, rabbit corneal, full-thickness wounds were stained, *en bloc*, with FITC-phalloidin and the f-actin organization analyzed using laser scanning confocal microscopy (LSCM). Using *en bloc* staining and the LSCM approach allowed us to analyze the entire wound without sectioning the tissue. Using a standard tissue sectioning approach, 14-day wounds

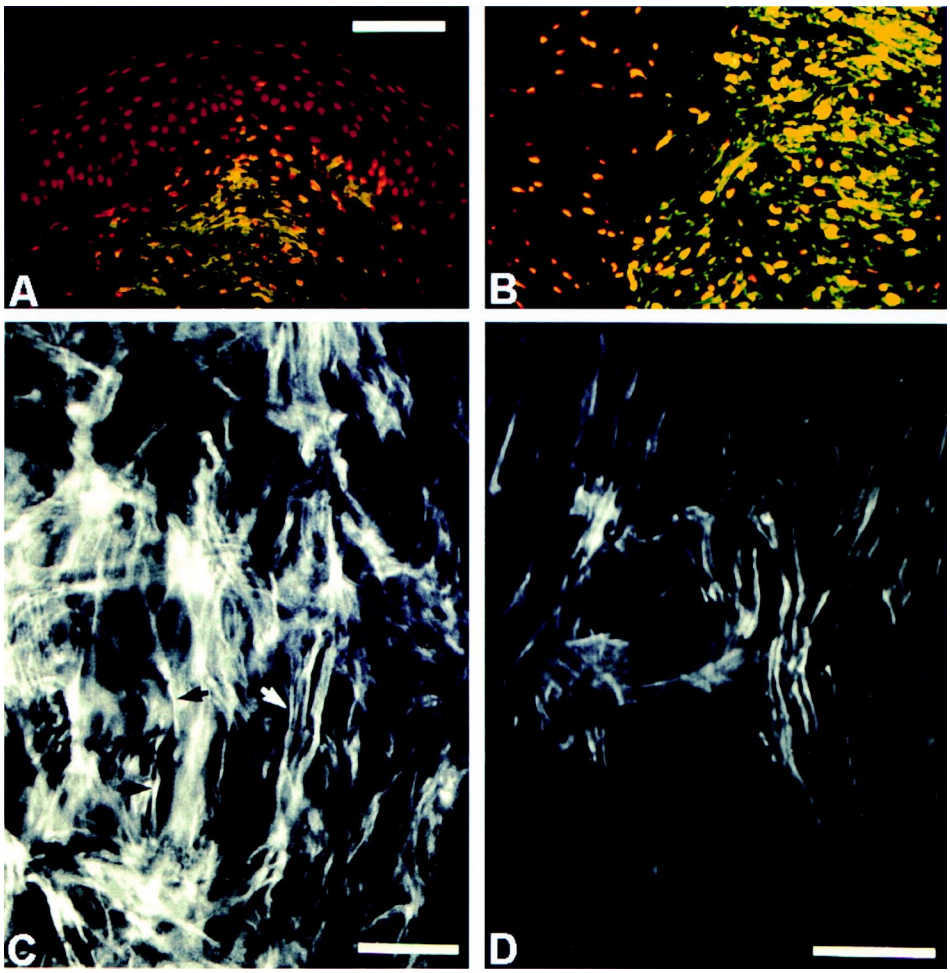

Fig. 10. (A) Low-magnification cross-section labeled for f-actin (green) and propidium iodide (red) showing light cortical f-actin staining of the epithelium, and intense staining of wound healing fibroblasts. (B) Image from a different area in the same cross-section as A. It appears in both A and B that the fibroblasts are organized into layers parallel to the wound surface. (C) A 14-day *en face* section, which suggests that the microfilament bundles (arrows) are oriented parallel to the long axis of the wound. (D) The f-actin distribution observed using *in situ* laser scanning confocal microscopy of *en bloc*-stained corneal tissue at 14 days after injury. The improved optical sectioning of LCM reduces the amount of out-of-focus information contributing to the image as compared to C. Bars: A, 100 μm, C,D, 25 μm. Taken from Petroll *et al.* (1993a) with permission.

showed fibroblasts organized into layers running parallel to the wound surface (Fig. 10A, B). Based on the propidium iodide staining of the cell nuclei, it was clear that the increase in staining was due primarily to increased organization of f-actin and not simply an increase in cell numbers. When viewed alone, the cross-sectional view of these layers led to the misinterpretation that the microfilament bundles were oriented directly *across* the wound, or perpendicular to the lateral wound margins. However, when wounds were sectioned or evaluated by LSCM in the *en face* plane (parallel to the wound surface), thin microfilament bundles appeared to be oriented *parallel* to the long axis of the wound and not across (Fig. 3C, D). This was exactly opposite to the orientation suggested from the cross-sectional data and demonstrated the importance of studying 3-dimensional systems using 3-dimensional techniques. Importantly, we concluded that cross-sectional results were misleading because the myofibroblasts organized into layers that gave the

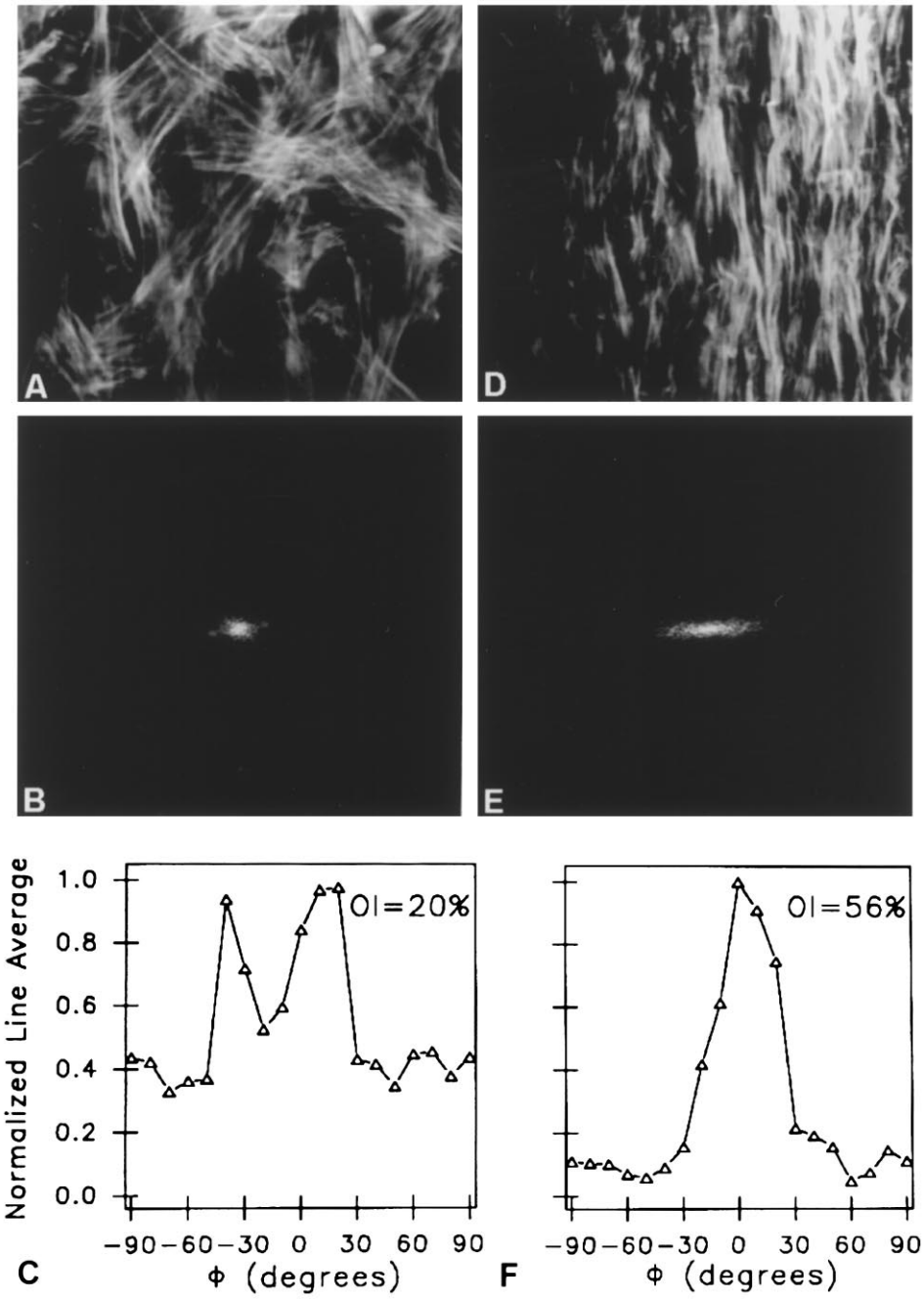

Fig. 11. Results of the analysis of microfilament bundle orientation at 10 (A, B and C) and 28 (D, E and F) days after injury. (A) The 10-day image of a corneal wound appeared to show bundles oriented at several different angles. (B) The Fourier Transform (FT) of image A produced a somewhat circular pattern with two angle bands at 20 and −40° which appeared slightly brighter than the rest, most likely corresponding to the parallel groups of stress fibers. (C) Line average plot of FT showed two peaks. The orientation index (OI) of 20% demonstrated that there was a slight overall alignment of bundles with the long axis of the wound (an OI of 0% = completely random distribution, 100% = completely parallel to long axis, −100% = completely perpendicular to the long axis). (D) The day 28 image of the corneal wound showed alignment of the bundles almost parallel to the long axis. (E) The FT produced an elliptical pattern, with the major axis at 90° to the long axis of the wound. (F) A plot of the line averages of the FT shows a sharp peak near 0°. The resulting OI of 56% confirmed that microfilament bundles are more oriented along the long axis than the 10-day image. Bar, 25 μm. Taken from Petroll *et al.* (1993a) with permission.

appearance of microfilament bundles spanning across the wound when viewed from the side.

Evaluation of microfilament bundles using 3-dimensional LSCM showed that the f-actin was randomly oriented at day 7 following injury but tended to align parallel to the long axis of the wound between day 10 (Fig. 11A) and day 14. By 28 days (Fig. 11D), the spatial organization appeared to be nearly parallel to the long axis of the wound. Using Fourier Transform (FT) analysis of microfilament bundle orientation, the organization of microfilaments was determined. An example of this analysis is provided in Fig. 11 for images from a 10 day and 28 day wound. In the

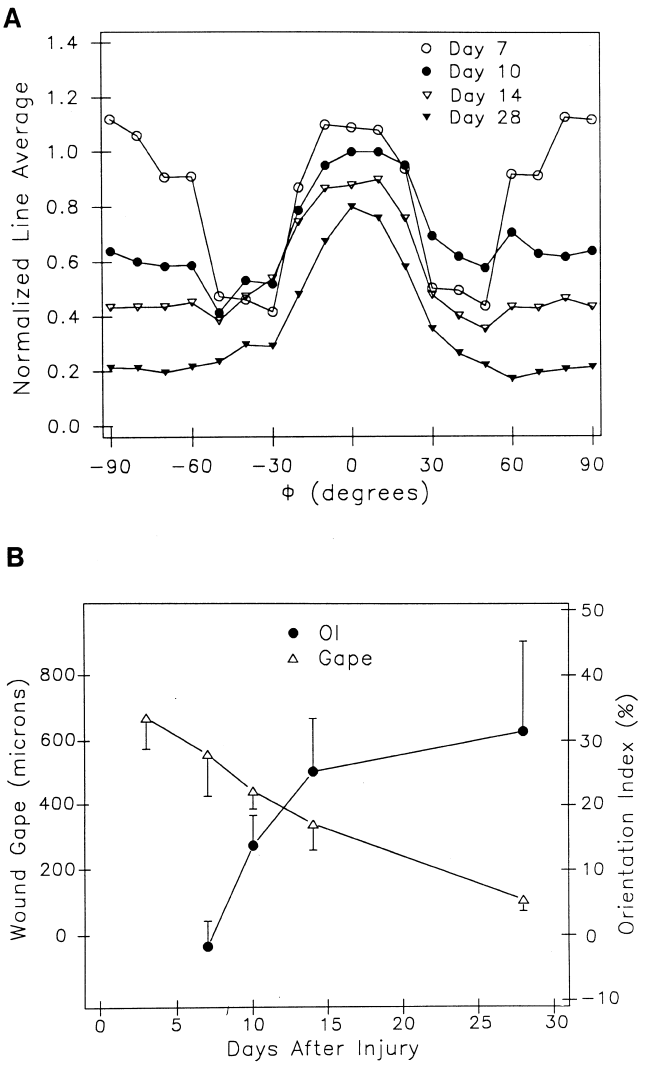

Fig. 12. Temporal change in the mean angle distribution of the FT line averages. A large population of microfilament bundles appeared oriented near the long axis (0°) of the wound was observed at all time points. However, "side lobes" were observed, which progressively decreased in relative magnitude over time. This suggested two separate populations of bundles, one oriented parallel to wound and across the wound. (B) A plot of the overall changes in bundle orientation (OI) compared to wound gape over time (error bars represent s.d.). OI calculations indicated that the stress fibers were randomly oriented at 7 days (OI = − 1.6) and progressively increased in orientation to 28 days after injury (OI = 31.4). Wound gape progressively decreased from 708 μm at 3 days after surgery to 130 μm at day 28. Taken from Petroll *et al.* (1993a) with permission.

image from the 10 day wound, FT produced a somewhat circular pattern with two angle bands at 20 and −40° that appeared slightly brighter than the rest. This resulted in a line average plot with two peaks (Fig. 11C). The orientation index (OI) of 20% indicated that there was a slight overall alignment of fibers with the long axis of the wound. FT analysis of an image from a 28 day wound produced an elliptical pattern (Fig. 11E), with the major axis at 90° to the long axis of the wound. A plot of the line averages calculated from the FT showed a sharp peak near 0° (Fig. 11F). The higher OI of 56% confirmed that the fibers were more aligned with the long axis than in the 10-day wound.

In evaluating the temporal changes in the FT line averages (Fig. 12A) from groups of animals at different times following injury, it was apparent that a large population of microfilament bundles oriented near the long axis of the wound at all time points. However, ''side lobes'' were observed which progressively decreased in relative magnitude over time. This was especially apparent at day 7, which suggested that two separate populations of fibers were present, one oriented along the wound, and one across the wound. OI calculations (Fig. 12B) showed that the microfilament bundles were more randomly oriented at day 7 (OI = − 1.6%) and progressively increased in orientation to 28 days (OI = 31.4%). These changes in orientation significantly correlated with the progressive decrease in wound gape from 708 μm at 3 days to 130 μm at day 28 ($r = -0.93$, $P < 0.05$).

Overall, this study demonstrated for the first time that microfilaments undergo a temporal reorientation during the process of wound healing that significantly correlated with the contraction of the wound. The orientation pattern also confirmed a unique contractile mechanism involved in the generation of tension within the wound. As shown in Fig. 13, microfilament bundles (stress fibers, *sf*) generate force vectors (F*sf*) which run parallel to the axis of the bundles and which can be broken down into two components: one oriented across the wound (F*sf,x*) and one oriented parallel to the wound (F*sf,y*). Since after incisional injury the greatest increase in wound gape occurs across the wound, the least resistance to shortening of wound gape ocurrs across the wound rather than along the wound (F*cy* > > F*cx*). Therefore, based on a force balance analysis, during contraction microfilament bundles tend to twist across the wound as they contract in response to the differences in resistance. This process would result in closure of the wound, as well as a more parallel orientation of the bundles along the long axis of the wound, comparable to the tightening of a shoelace.

3.2. Temporal Characteristics of Corneal Myofibroblasts

Although the above studies indicated that microfilament bundles showed a temporal reorientation during the process of wound healing, little was known about the overall cellular organization of myofibroblasts within wounds. Furthermore, how any organizational structure was involved in the temporal translocation of force from individual cells to the wound margins was not clear. In order to gain better insight into this question we evaluated the temporal, 3-dimensional changes in myofibroblast organization using *in vivo* confocal microscopy which provided a non-invasive, dynamic, 3-dimensional view of the tissue and cell organization (Jester *et al.*, 1992a; Petroll *et al.*, 1992a).

Using the rabbit model of full-thickness incisional injury, healing of corneal wounds were evaluated daily for 2 to 4 days by *in vivo* confocal microscopy prior to sacrifice after injury at day 7, 14, 21 and 28. In general, keratocytes appeared to become activated adjacent to the wound at about 3 days after injury (Fig. 14A, open arrow). Activated keratocytes were detected by their increased reflectivity of light, which revealed details of the cellular processes that appeared to extend toward the wound. Migration of activated keratocytes into the wound began around day 4, and continued till about day 10 to 14 when the anterior portion of the wound was completely populated by myofibroblasts. Even at the earliest stages of cell migration, activated keratocytes and myofibroblasts appeared to maintain cell–cell contact through the extension of thin, broadly spaced, pseudopodial processes (Fig. 14B, arrows). Once inside the wound, myofibroblasts

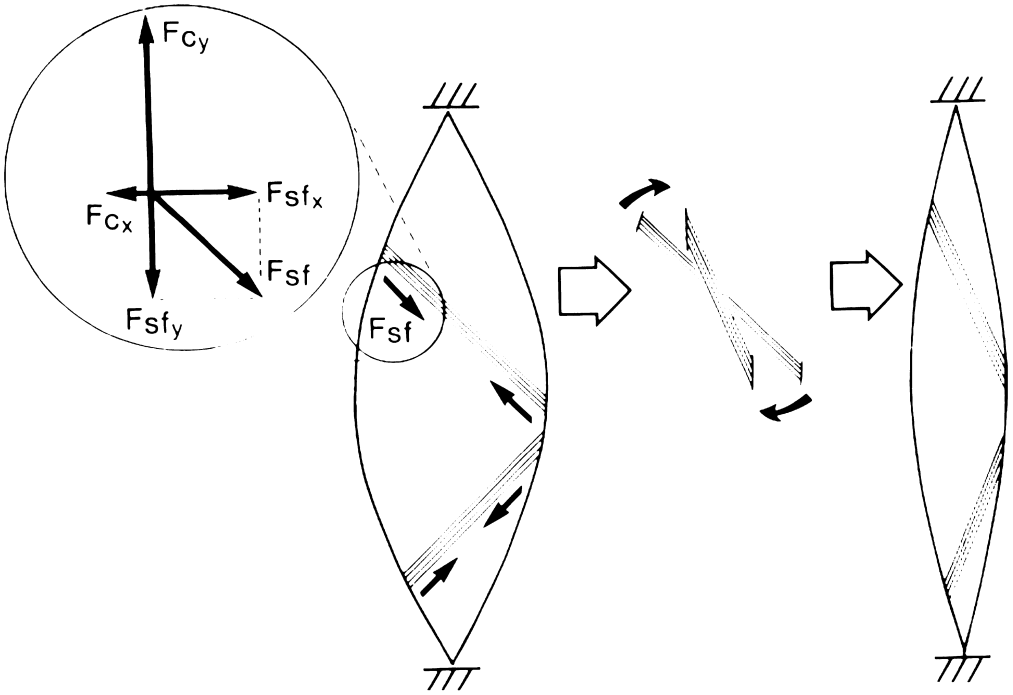

Fig. 13. A sketch of the contractile mechanism by which microfilament bundles (stress fibers, *sf*) become oriented along the long axis of the wound during wound contraction. In this contractile model, bundles generate force parallel to the axis of the microfilament bundle. From a biomechanical standpoint the axial force vector (F*sf*) can be broken down into two components, one oriented across the wound (F*sf,x*) and one oriented parallel to the wound (F*sf,y*). Since after incisional injury the greatest increase in wound gape occurs across the wound, there is much less resistance to shortening of wound gape across the wound than along the wound (F*cy* > > F*cx*). Therefore, during contraction, microfilament bundles tend to twist across the wound as they contract in response to the difference in resistance. Taken from Petroll *et al.* (1993a) with permission.

maintained their interconnected organization but the processes appeared to become thicker and align more parallel to the wound margins (Fig. 14C, arrows). By 28 days, the wound had undergone marked contraction and both wound margins were visible in the same field of view (Fig. 14D, curved arrows).

Using digital imaging techniques the three-dimensional organization of myofibroblasts was identified. A series of 10 to 15 optical slices separated by 4 μm in the z-axis were collected at various times after injury (Fig. 15). The z-series suggested that cells showed an extensive interconnectivity and branching throughout the wound, forming a 3-dimensional meshwork. Using immunofluorescent staining of conventional frozen sections (Fig. 16) the junctions between myofibroblasts showed staining for connexin 43 (A and B), a gap junction protein (Beyer *et al.*, 1989), suggesting that cells within the wound were coupled. Additionally, pseudopodial extensions from myofibroblasts toward adjacent keratocytes at the wound margin also showed staining for connexin 43 suggesting that the wound and cornea remained physiologically coupled during wound healing. Work by Watsky (1995) has shown that these connections are functional physiologically.

To assess the temporal changes in myofibroblast organization, 3-dimensional data was collected in the same region of the wound at 24-hour intervals. Individual cells were first identified and mapped to nonmoving fiducial points such as fixed-edge patterns and later traced, segmented, and reconstructed 3-dimensionally (Fig. 17). Using this approach the movement of

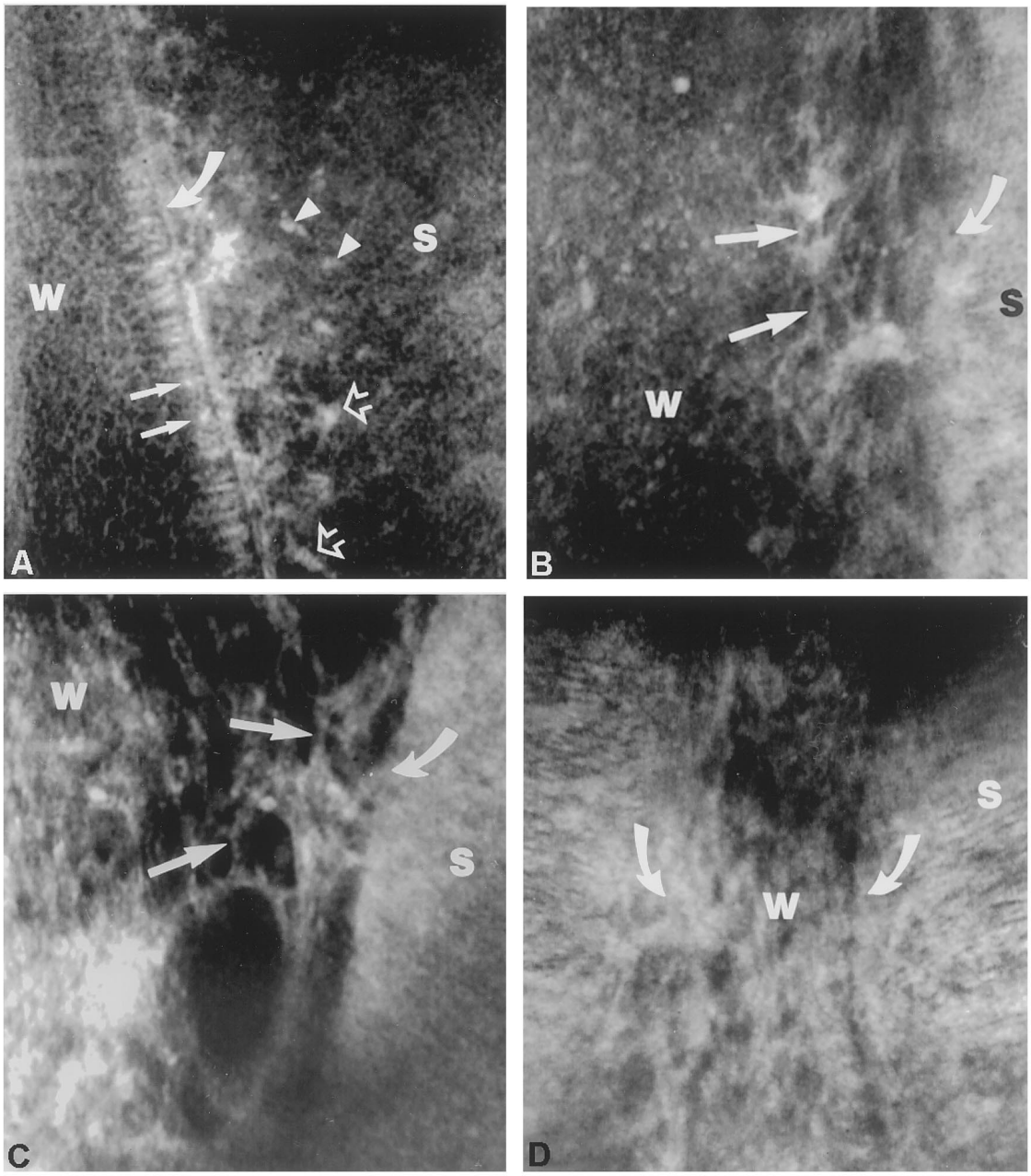

Fig. 14. *In vivo* confocal micrographs taken from the same eye at day 3 (A), 7 (B), 10 (C), and 28 (D) showing the wound area (W), undamaged stroma (S) and the wound margin (curved arrow). At day 3 (A) the wound margin is lined by epithelium. Adjacent to the stroma, basal epithelial cells (arrows) appear highly reflective, while the in the stroma, note the presence of inflammatory cells (arrowheads) and keratocyte nuclei (open arrows) showing early activation and the appearance of the cell body. At day 7 (B) activated keratocytes have migrated into the wound and appear to be interconnected by thin cellular processes (arrows). At day 10 (C), cell process (arrows) appear to be thicker and are aligned predominantly parallel to the wound margin. At day 28 (D) wound contraction has led to near re-apposition of the wound margins (curved arrows). (Image width = 400 μm) Taken from Jester *et al.* (1995) with permission of the Cambridge University Press.

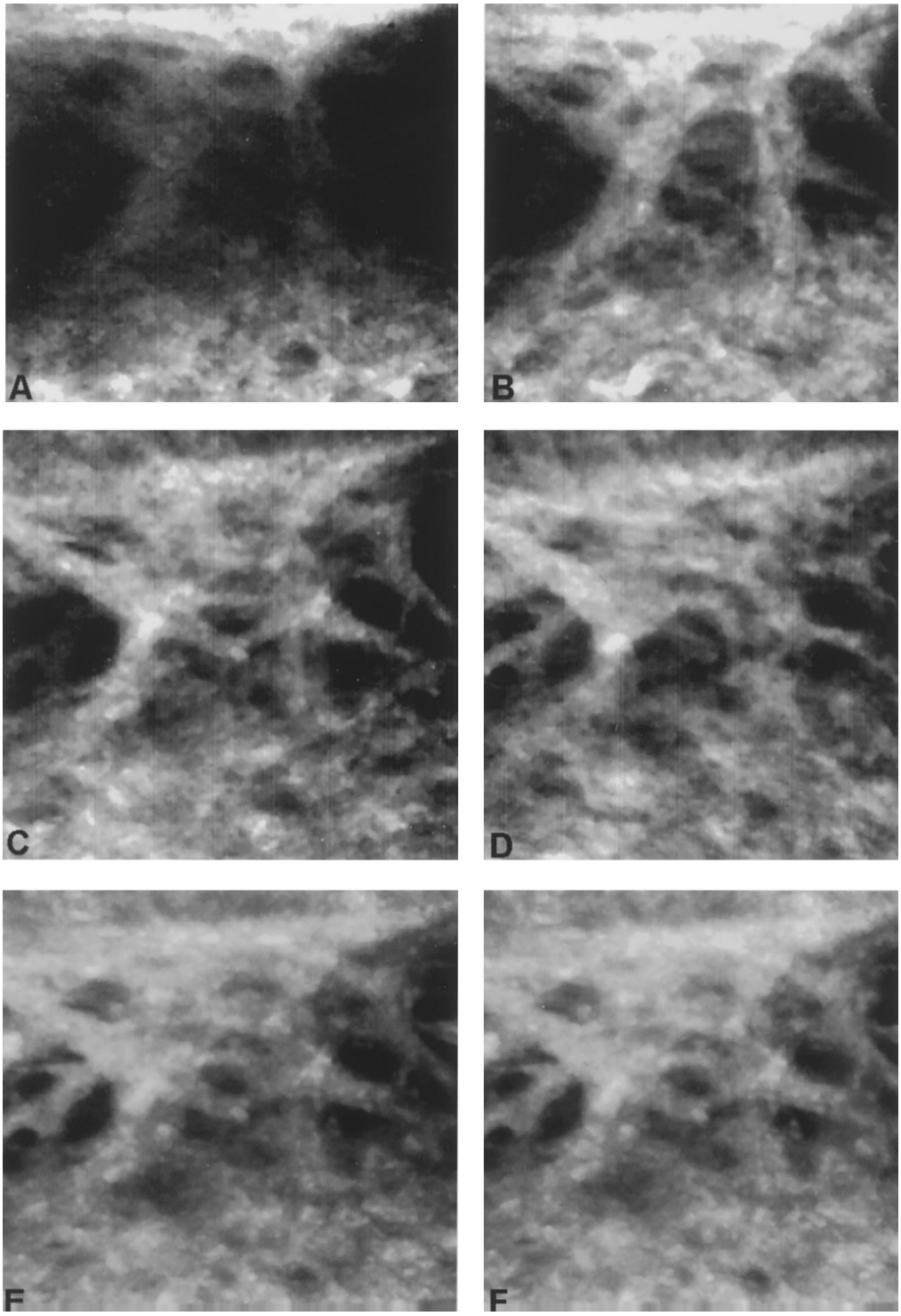

Fig. 15. *In vivo* confocal z-series of images (A–D) and stereo pair (E and F) of myofibroblasts adjacent to the wound at 7 days after injury. 2-Dimensional images (A–D) focus from the anterior cornea (A) into the wound (D) showing an extensive, interconnected meshwork of myofibroblasts. The stereo pair, (E and F) more dramatically illustrates this 3-dimensional interconnectivity. (Image width = 400 μm). Taken from Petroll *et al.* (1993b) with permission from the Royal Microscopical Society.

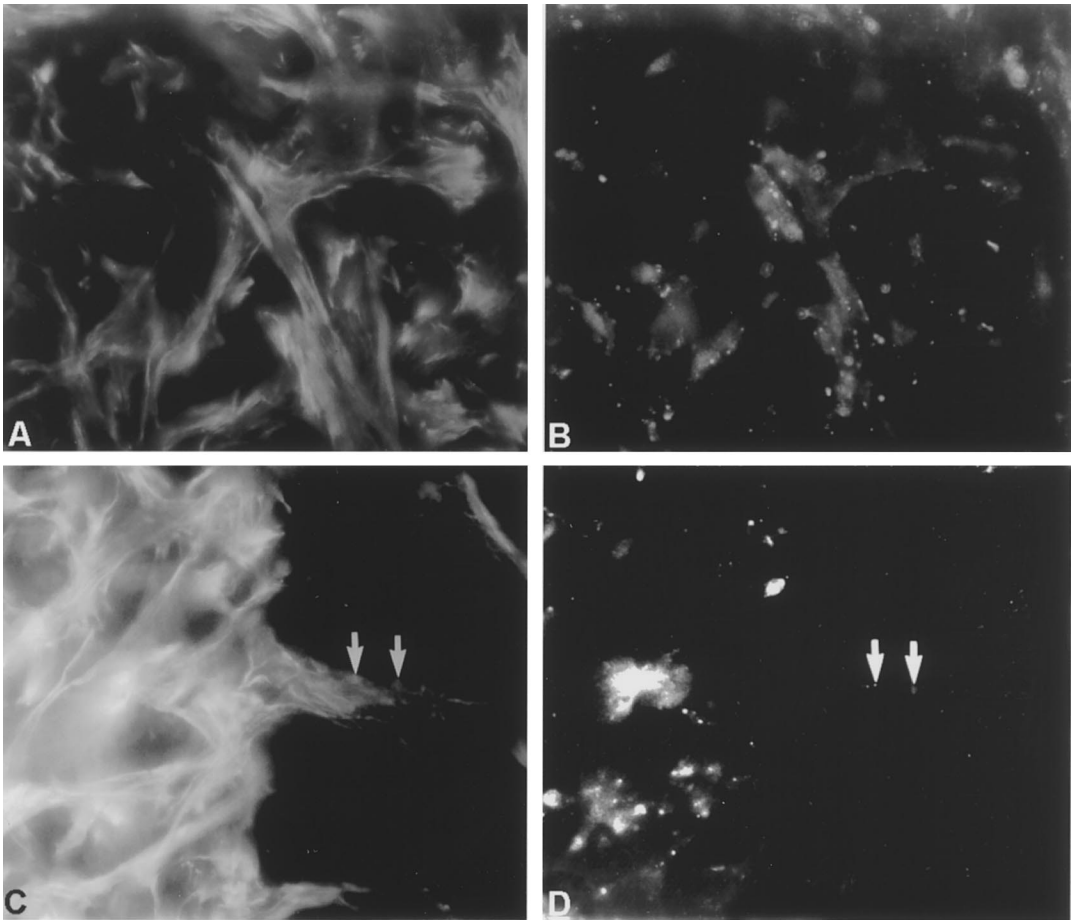

Fig. 16. Co-localization of phalloidin staining (A, C) with anti-connexin 43 staining (B,D) in wound fibroblasts, 7 days after injury. Fibroblasts in the center of the wound (A, B) and at the wound margin (C, D) showed prominent expression of connexin 43. Cells adjacent to the wound (C, D, arrows) also appeared to show positive staining, suggesting interconnection of the wound fibroblasts with adjacent normal keratocytes. (Original magnification, ×450). Taken from Jester *et al.* (1995) with permission of the Cambridge University Press.

individual cells appeared to involve predominantly cell elongation along and reorientation *towards* the axis of the wound *rather than across* the wound. Furthermore, these findings were consistent with the earlier work showing the orientation of microfilament bundles toward the wound margins.

Additional co-localization studies (Fig. 18) also showed that microfilament bundles, stained with phalloidin, co-aligned with extracellular collagen type I (A and B) and fibronectin (C and D) which were linked by the surface membrane receptor, $\alpha 5\beta 1$ integrin (E and F). Overall, these findings indicate that wound myofibroblasts establish and maintain an interwoven network of coupled cells and extracellular matrix, collagen and fibronectin, forming a 3-dimensional "shoe string-like" structure. In such a structure, muscle-like contraction of actin filaments results in tightening of the interconnected cellular and matrix network similar to tightening of a shoe lace. This results in alignment of cells, cellular processes and extracellular matrix, parallel to the wound margins. Importantly, the presence of gap junction-associated protein and functional gap junctions suggests that cell–cell communication may play a critical role in regulating the sequence of contractile events.

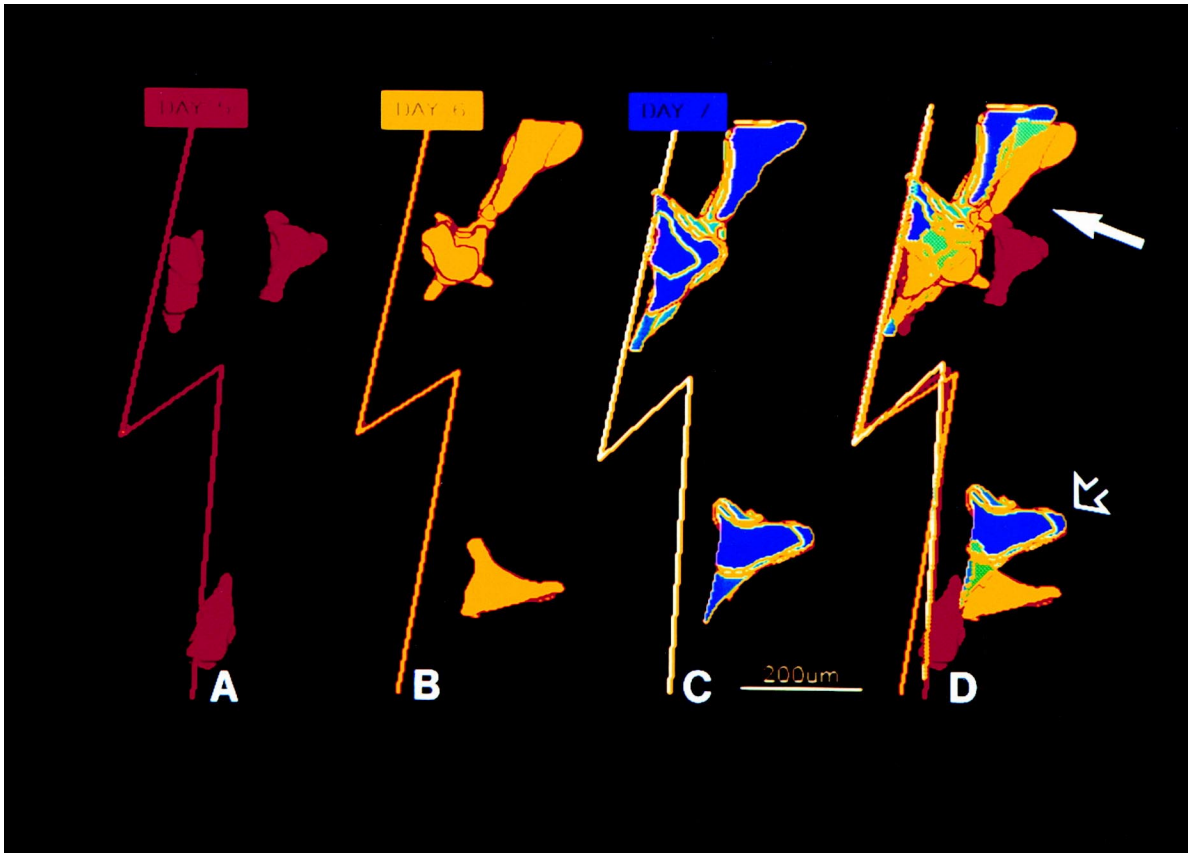

Fig. 17. Three-dimensional reconstructions of myofibroblasts were obtained by extracting outlines of cells in individual 2-dimensional images prior to volume rendering using the depth gradient shading algorithm in ANALYZE (Medical Adventures Inc, Rochester, MN) from day 5 (A), 6 (B) and 7 (C). Movement of cells was determined by aligning separate data sets to the wound margin. Line indicates wound margin separating wound from intact stroma as detected in the first optical slice. Composite (D) represents an overlay of the wound margins in the volume rendered images showing cell elongation (arrow) and reorientation (open arrow). Bar, 200 μm. Taken from Jester *et al.* (1995) with permission of the Cambridge University Press.

4. THE PROCESS OF CORNEAL MYOFIBROBLAST TRANSFORMATION

In studying myofibroblast transformation, many of the characteristics of myofibroblasts appeared to be expressed by keratocytes in culture. Although culture models provided an attractive alternative to *in vivo* studies, particularly regarding the ease of performing biochemical and molecular analyses, it was important to establish that the pathway of *in vitro* myofibroblast transformation was similar to or closely paralleled that observed in corneal wounds. In order to establish this similarity, we have more clearly identified the phenotypic characteristics of the *in vivo* corneal myofibroblast concerning the expression and organization of muscle proteins and the contractile apparatus. Secondly, we have attempted to characterize the structural characteristics of the normal quiescent keratocyte as relates to organization of contractile proteins, including f-actin, myosin, α-actinin, fibronectin, and $\alpha 5\beta 1$ integrin. We then evaluated several culture models of myofibroblast transformation. We believe that these studies clearly establish at least one pathway for the induction of myofibroblast transformation of corneal keratocytes that appears to mimic the *in vivo* transformation process.

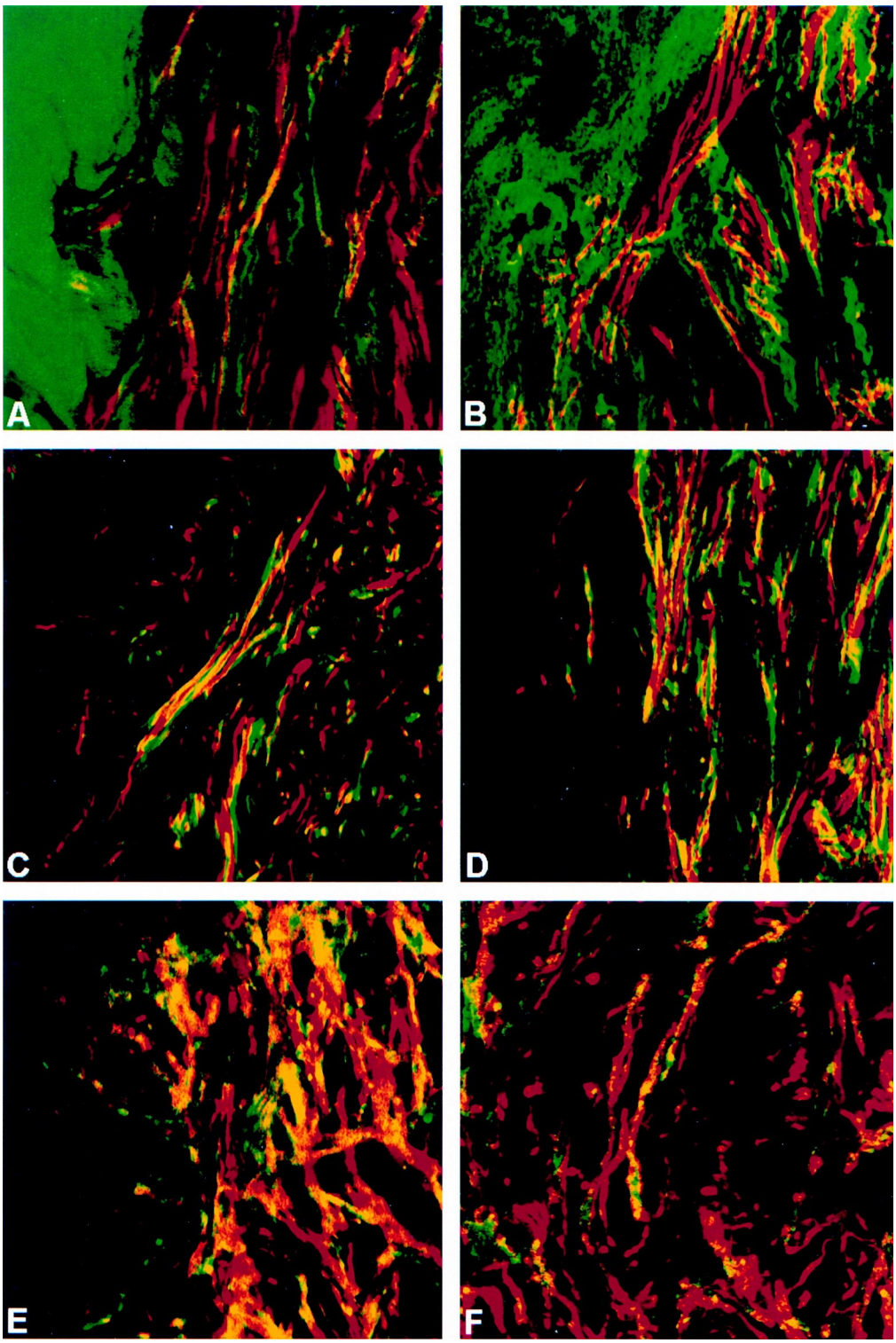

Fig. 18. LSCM co-localization of actin filament bundles (red) and extracellular matrix and matrix receptors (green) in 7 day (A, C, E) and 14 day (B, D, F) rabbit full thickness corneal wounds. AB, co-localization with collagen type I. CD, co-localization with fibronectin. EF, co-localization with $\alpha 5\beta 1$ integrin. (Original magnification, ×625).

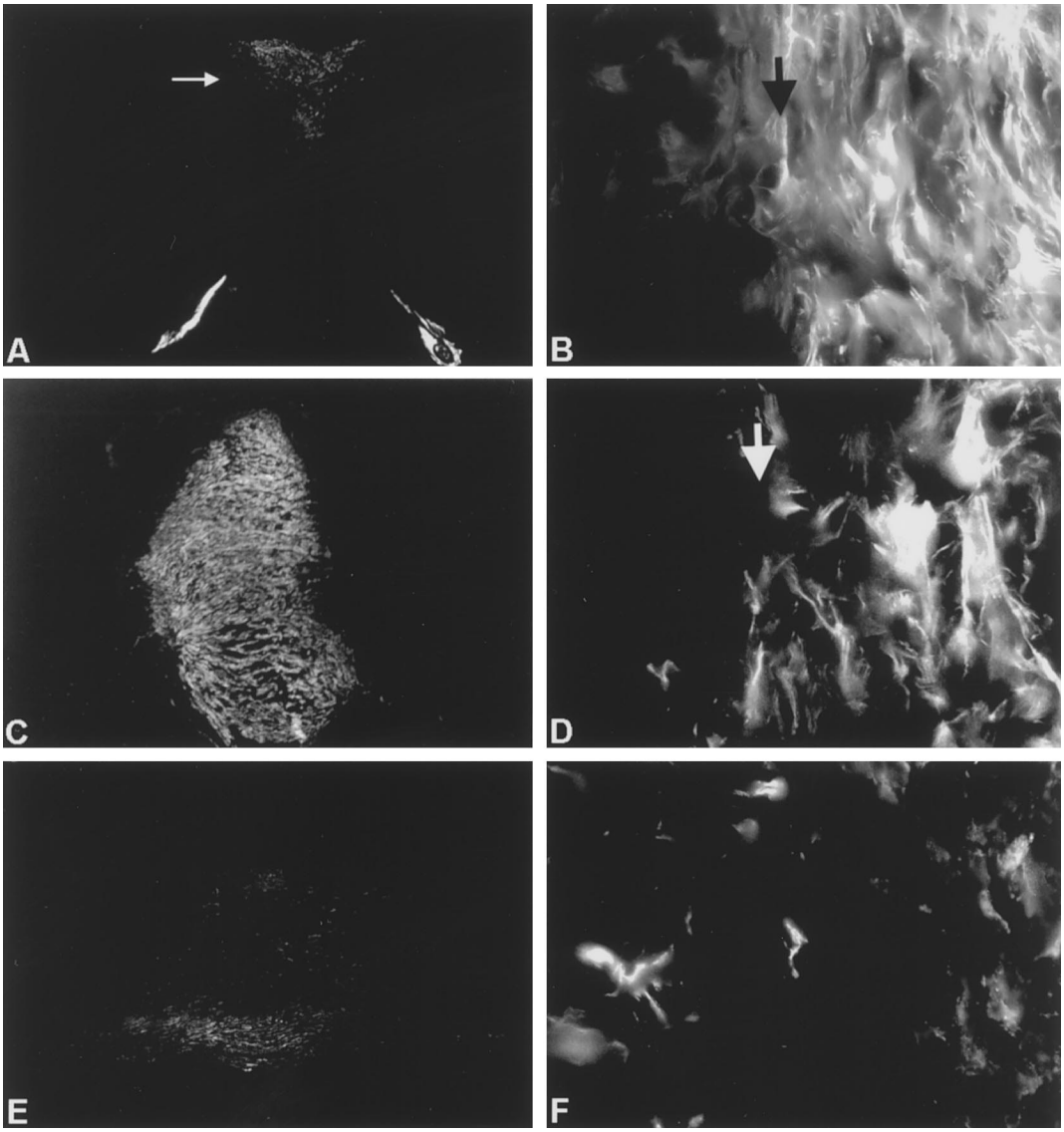

Fig. 19. Immunofluorescent staining of 7-day (A, B), 14-day (C, D), and 28-day (E, F) rabbit corneal full-thickness wound by monoclonal antibodies specific for human α-SMA. (A) Cells within the anterior part of the wound (arrow) show intense staining. (B) *En face* section from the anterior of the wound (arrow indicates wound margin). Only cells within the wound appeared to stain. (C) Cross-section of 14-day wound showing that the entire wound is positive for α-SMA. (D) *En face* sections showed bundles of α-SMA staining, restricted to the wound (arrow indicates wound margin). (E) Cross-section of 28-day wound showed staining primarily in the posterior part of the wound and little staining anteriorly where the wound has already contracted. (F) *En face* section from anterior of 28-day wound showed diffuse staining of α-SMA, indicating breakdown of stress fibers in the wound. Also at this time point, cells outside the wound margin appeared to stain for α-SMA indicating possible migration of cells out of the wound. (Original magnification; A, C, E, ×52; B, D, F, ×720). Taken from Jester *et al.* (1996) with permission from the Association for Research in Vision and Ophthalmology.

4.1. The *In Vivo* Myofibroblast Phenotype

In recent years, the structural features of myofibroblasts has been further extended to include the expression of a smooth muscle specific protein, α-actin (Darby *et al.*, 1990). Expression of α-SMA has been used by various investigators as a chemical marker for myofibroblast transformation

(Desmouliere *et al.*, 1992a,b). Although earlier isoelectric focusing studies failed to demonstrate the presence of α-SMA, more sensitive analyses using monoclonal antibodies specific of α-SMA (Skalli *et al.*, 1986) have more recently shown that alkali and incisional injury to the cornea are associated with expression of α-SMA during wound healing (Ishizaki *et al.*, 1994).

Using these monoclonal antibodies, the temporal expression and localization of α-SMA in full-thickness, incisional wounds of the rabbit have been established and correlated to wound contraction. Expression of α-SMA was first detected in wound healing fibroblasts as they migrated into the wound as early as day 3 but only a few cells were present in the wound at that time. By day 7 after injury (Fig. 19A) fibroblasts present in the anterior (arrow) wound showed intense staining for α-SMA. When tissue blocks were sectioned *en face*, staining of α-SMA appeared to be organized into bundles, similar to stress fibers, and aligned parallel to the plane of the section (Fig. 19B). At 14 days, anti-α-SMA staining was present throughout the wound but appeared to be confined to within the borders of the wound (Fig. 19C, D). From day 28 to 42, after most of the wound contraction had occurred, anti-α-SMA staining had diminished and was limited to the posterior portion of the wound (Fig. 19E). The loss of α-SMA staining also appeared to be related temporally to the breakdown of stress fibers within the wound (Fig. 19F). Overall, there was a progressive wave of expression of α-SMA, beginning first in the anterior wound and progressing posteriorly; exactly paralleling the temporal invasion of the wound by fibroblasts and the concomitant onset and completion of wound contraction.

Interestingly, expression of α-SMA appeared to be almost exclusively localized to cells within the wound. Fibroblasts adjacent to the wound but residing within undamaged corneal stroma contained f-actin stress fibers but did not express α-SMA. The strict localization of α-SMA to within the wound was further confirmed in DTAF-stained corneas where the original corneal stroma was stained by the covalently bound fluorescent dye, marking the original wound margins (Fig. 20A). Staining of α-SMA actin by rhodamine-conjugated goat anti-mouse IgG showed that α-SMA was strictly limited to the wound tissue (Fig. 20B) and was not detected in the intact stroma.

Besides the clear indication that corneal myofibroblasts uniquely express α-SMA, the most important finding concerning the myofibroblast transformation process was the unexpected finding that α-SMA expression was *exclusively* limited

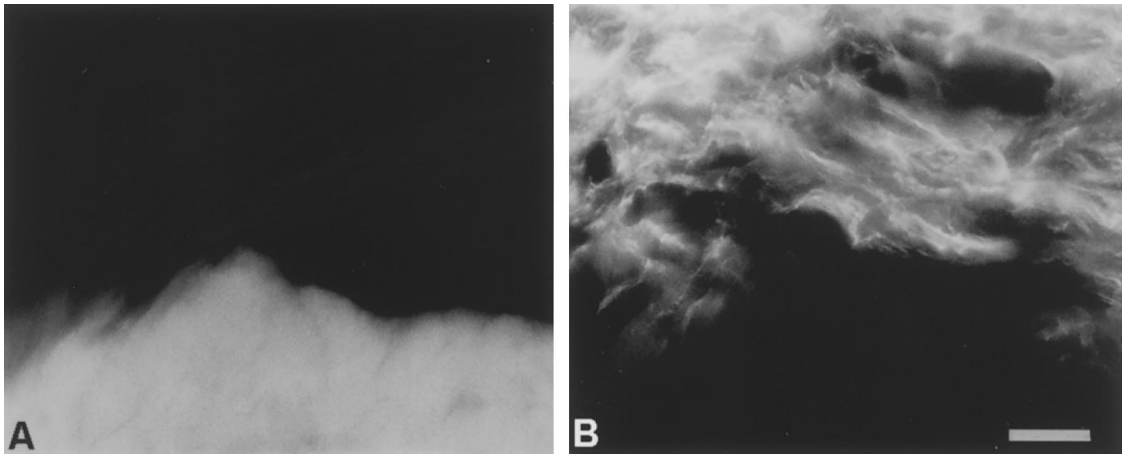

Fig. 20. (A) Cornea stained with DTAF at the time of injury showed marked fluorescent staining of the wound margin at 14 days after injury. (B) anti-α-SMA staining showed α-SMA localized strictly to the wound tissue, with no α-SMA staining adjacent to the wound. Bar = 20 μm. Taken from Jester *et al.* (1996) with permission from the Association for Research in Vision and Ophthalmology.

to cells within the wound. Although staining with phalloidin identified adjacent cells containing stress fibers and microfilament bundles, only myofibroblasts within the wound expressed α-SMA. This observation supports the hypothesis that myofibroblasts are derived from the transformation of adjacent quiescent keratocytes since migration of α-SMA containing cells from the limbus would have been easily detected. More importantly, however, the close association

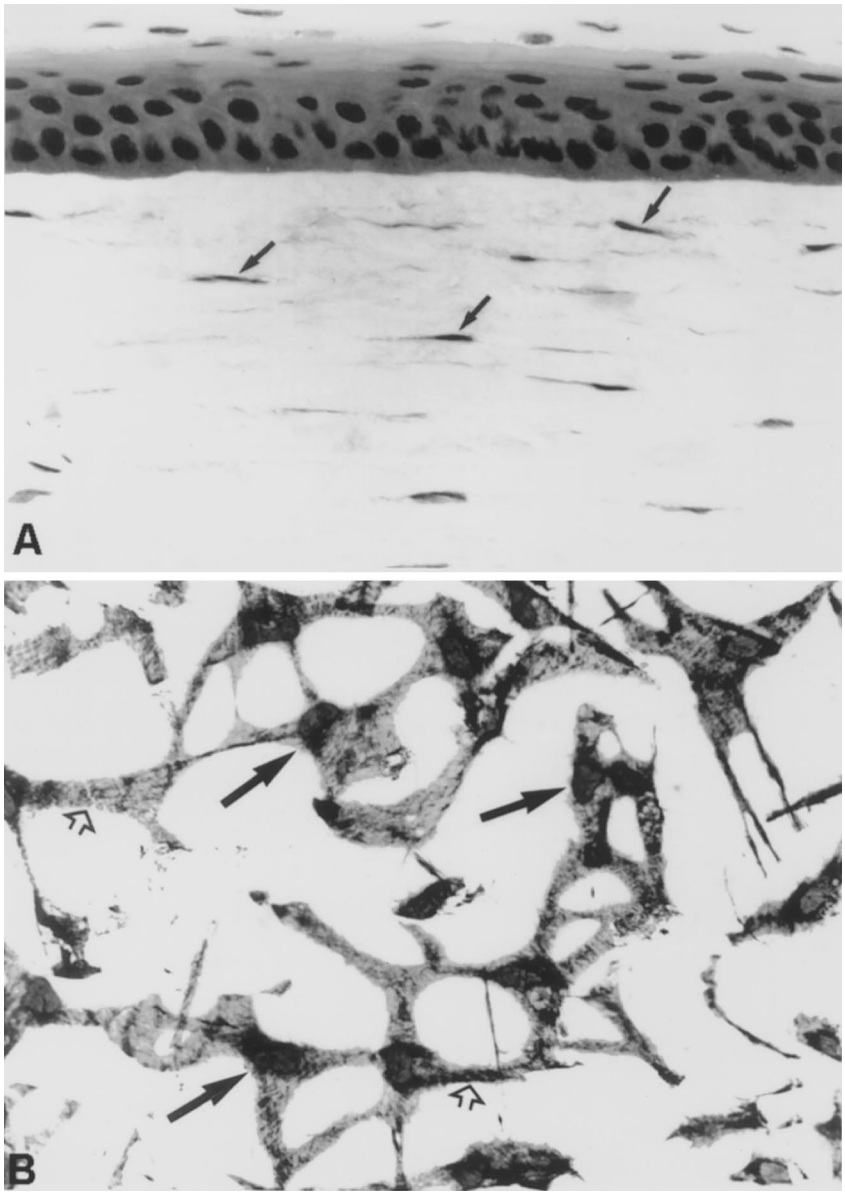

Fig. 21. Normal cat cornea cut in (A) cross-section and stained with hematoxylin and eosin and (B) *en face* section stained with gold chloride. In cross-section, keratocytes appear as a sparse population of cells (A, arrows) while in *en face* section keratocytes comprise a network of broad cells that are interconnected by cellular processes (B, open arrows) extending from a central cell body containing the nucleus (B, arrows). (Original magnification; A, ×512; B, ×329). Taken from Jester *et al.* (1994) with permission from the Association for Research in Vision and Ophthalmology.

between myofibroblast transformation and the newly developing wound tissue suggests that specific or unique environmental factors "inside" the wound play a critical regulatory role in the transformation process. While soluble factors such as heparin and TGFβ (Desmouliere *et al.*,

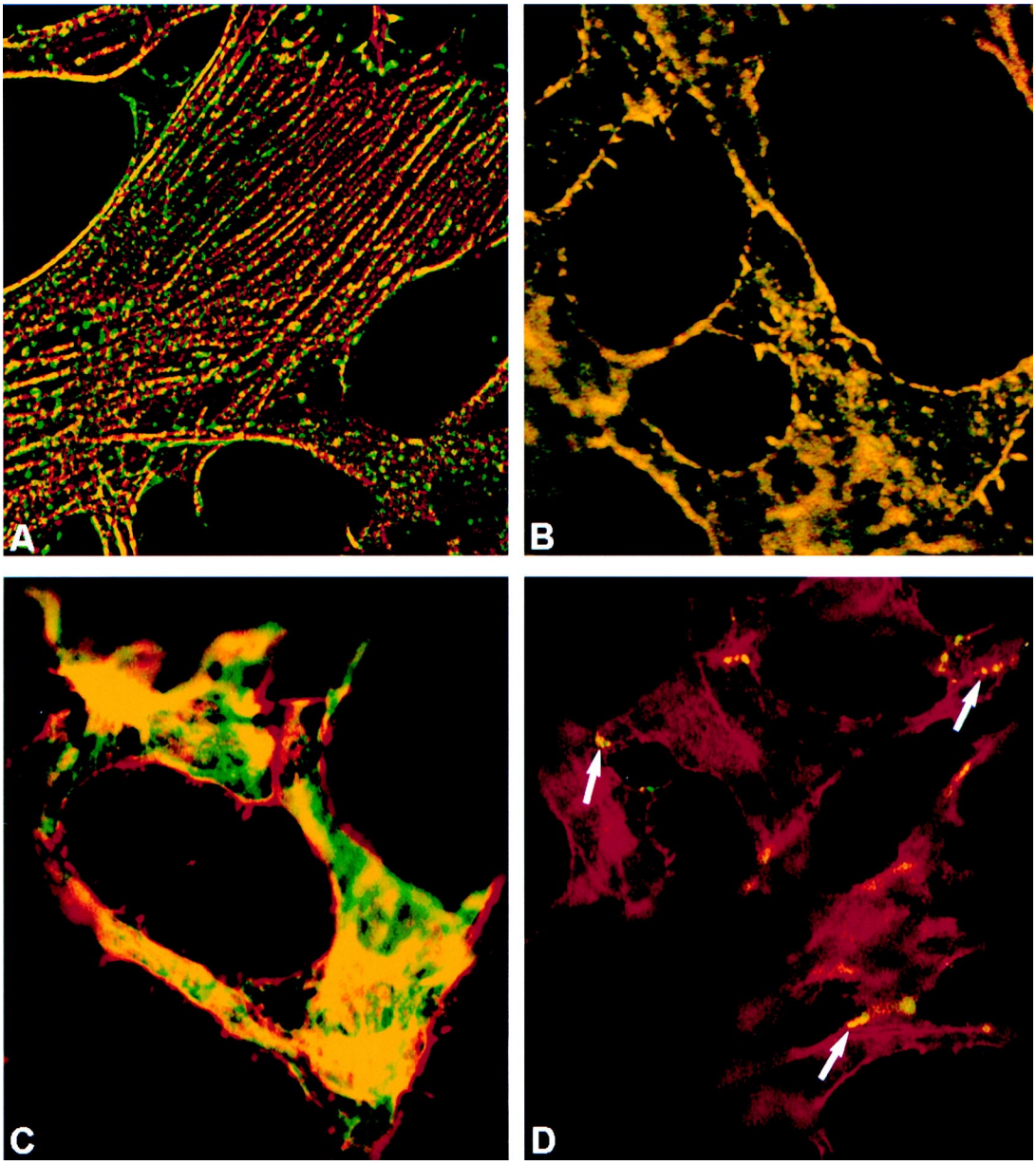

Fig. 22. LSCM images of cultured (A) and *in situ* (B–D) keratocytes stained for the presence of myosin (A, B, D; red), α-actinin (A, B; green), f-actin (C, red), vimentin (C, green) and connexin 43 (D, green). In cultured keratocyte (A) myosin and α-actinin are localized along f-actin containing stress fibers, but appear to decorate the stress fibers in alternating beads. In the *in situ* keratocyte (B), myosin and α-actinin are co-localized as indicated by the overlapping of red and green signals to produce a yellow signal. Co-localization of f-actin and vimentin (C) showing separate red (f-actin) and green (vimentin) signals coming from the cell cortex and intracellular cytosol respectively. Co-localization of myosin and connexin 43 (D) shows connexin to be localized to sites of cell–cell contact. Taken from Jester *et al.* (1994) with permission from the Association for Research in Vision and Ophthalmology.

1992b, 1993) may induce expression of α-SMA in culture, soluble, diffusible factors do not appear to act alone in this process.

4.2. The Keratocyte Phenotype

Many studies have used tissue culture models to define the biosynthesis and functional characteristic of the corneal keratocyte. Normal keratocytes in culture, however, acquire characteristics similar to activated keratocytes and myofibroblasts; particularly regarding growth up-regulation, migration, and development of stress fibers. Although there are clear difference between tissue culture and wound healing the presence of stress fibers, focal contacts containing α5β1 integrin, and the expression of α-actinin suggests that tissue culture results in activation of keratocytes that mimics wound healing. To begin to understand myofibroblast transformation, it is then first important to differentiate clearly the quiescent from the activated wound healing corneal keratocyte phenotype.

First, the normal, quiescent keratocytes, as detected by routine histologic processing and sectioning, appear as a sparse population of flat cells residing between collagen lamellae (Fig. 21A, arrows). If the corneal tissue is cut *en face* or along the lamellar plane by routine or optical sectioning, the keratocytes show a higher density in the anterior cornea immediately below the epithelium than in the middle of the stroma (Muller *et al*., 1995; Petroll *et al*., 1995). Keratocytes also appear as broad cells forming an elaborate network of processes that are interconnected (Muller *et al*., 1995). These cellular processes have been shown to be sites of intercellular tight and gap junctions (Fig. 21B, open arrows) (Hasty and Hay, 1977; Ueda *et al*., 1987; Nishida *et al*., 1988). This is in distinct contrasted to the spindle shaped, fibroblastic appearance of keratocytes grown in culture.

As mentioned earlier, tissue culture also induces the organization of f-actin into stress fibers. Localizing along the stress fiber bundles are the major actin binding proteins, myosin (Fig. 22A, red) and α-actinin (Fig. 22A, green) which appear adjacent to each other along the stress fiber but do not directly overlap. A similar organizational distribution is not detected in normal keratocytes within tissues. Rather, keratocytes *in situ* show a cortical distribution of f-actin which is directly co-localized with overlapping myosin (Fig. 22B, red) and α-actinin (Fig. 22B, green). The cortical distribution of f-actin is more easily observed when f-actin (Fig. 22C, red) is co-localized with vimentin (Fig. 22C, green), an intermediate filament protein that is located intracellularly. Keratocytes in culture and *in situ* also show staining for the presence of connexin 43, the gap junction protein. However, *in situ* keratocytes show localization of connexin 43 (Fig. 22D, green) at defined sites of cell–cell attachment as indicated by anti-myosin co-localization (Fig. 22D, red).

Another important difference is the finding that the fibronectin receptor, α5β1 integrin, is localized to focal adhesion structures at the termini of stress fibers in cultured keratocytes, but in a diffuse, punctate staining pattern in *in situ* keratocytes suggesting the absence of focal adhesion. Studies by Masur *et al*. (1993) indicate that quiescent keratocytes do not express α5 integrin which is up-regulated when cells are grown in culture. The finding of punctate staining *in situ* probably reflects binding of anti-α5β1 antibodies to other β1 integrin containing adhesion structures. Additionally, fibronectin is not detected adjacent to *in situ* keratocytes.

Overall, these findings suggested that in the normal keratocyte, f-actin, myosin, and α-actinin constitute a major component of the cortical or submembranous cytoskeleton. On the other hand, culture of keratocytes appears to results in an alternation of the normal cell architecture with the formation of stress fibers and the development of actin binding structures similar to the contractile apparatus identified in wound healing myofibroblasts. These tissue culture induced phenotypic changes in the keratocyte appear to mimic the *in vivo* myofibroblast transformation process and therefore bring into question the use of standard cell culture to study the process of keratocyte transformation.

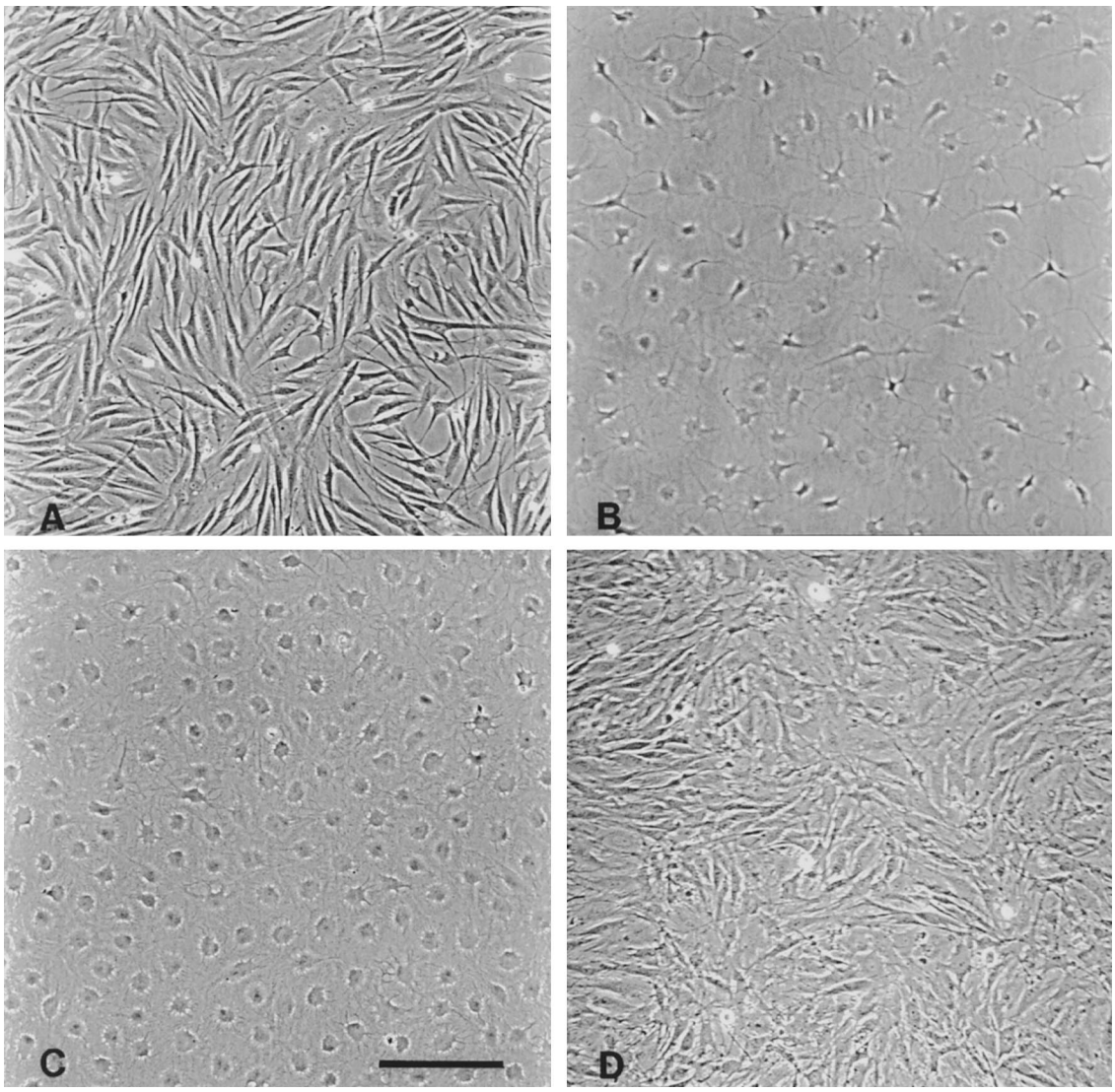

Fig. 23. Phase contrast micrographs of rabbit corneal keratocytes cultured for 7 days with (A) 10% serum, (B) serum-free or serum-free supplemented with (C) bFGF (10 ng/ml) and (D) $TGF_{\beta 1}$ (1 ng/ml). Bar = 200 μm. Taken from Jester *et al.* (1996) with permission.

4.3. Induction of Myofibroblast Transformation in Cultured Corneal Keratocytes

Since growth of keratocytes under standard culture conditions appeared to mimic, in part, the activation of *in situ* keratocytes to myofibroblasts, a question arose as to whether cultured keratocytes exhibited other features of myofibroblast transformation. Specifically, α-SM actin expression has been used as a biochemical marker for myofibroblast transformation in other cell culture systems (Desmouliere *et al.*, 1992a,b). Isolation of quiescent dermal fibroblasts and growth under standard culture conditions containing serum has identified a small (1–10%) population of cells which express α-SM actin, suggesting that fibroblasts are a heterogeneous population (Desmouliere *et al.*, 1992a). Selective expansion of α-SM actin positive cells has also been demonstrated when cultures are exposed to

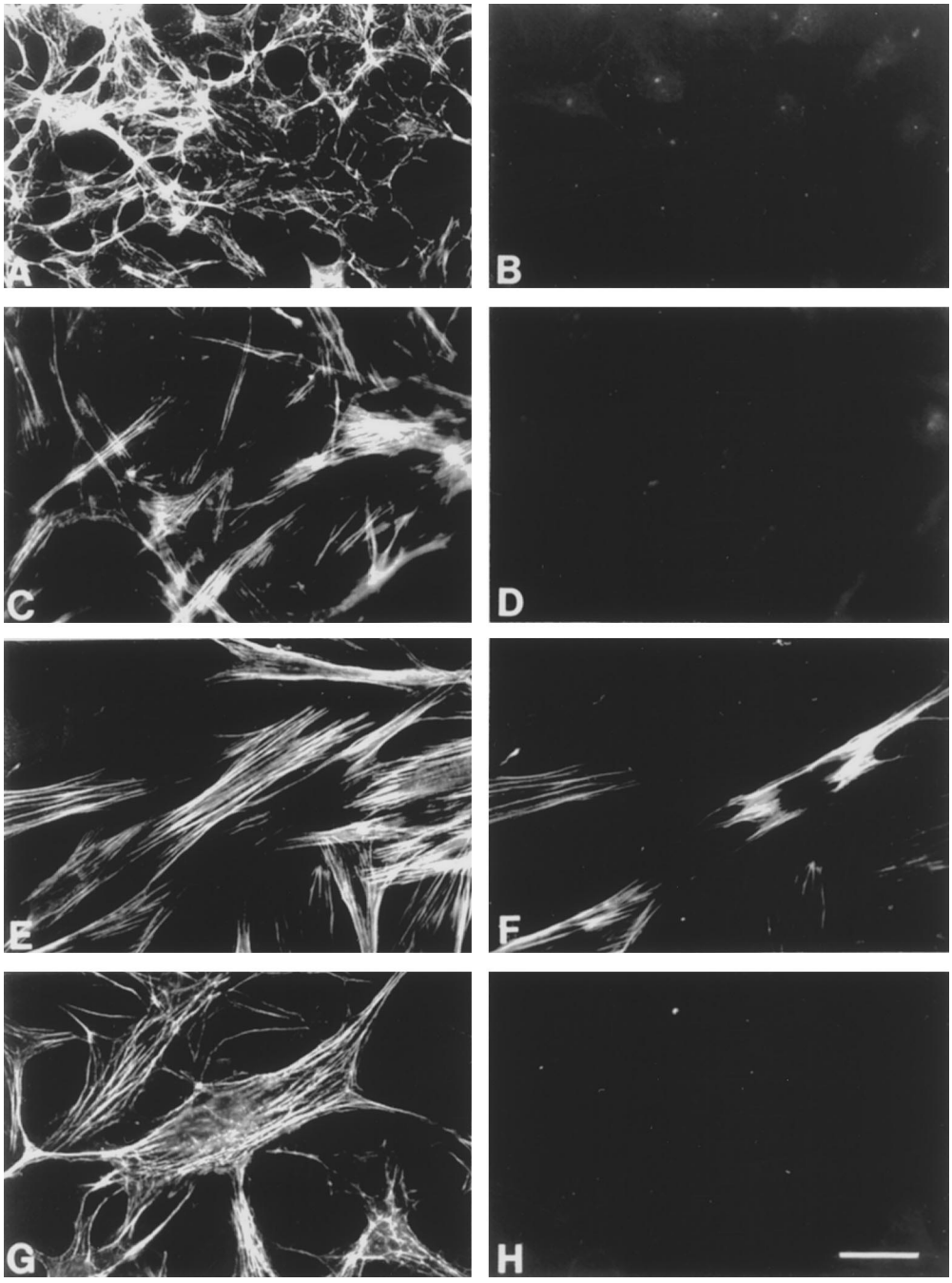

Fig. 24. Primary rabbit corneal keratocytes cultured in the absence of serum (A and B), or serum-free conditions supplemented with 10 ng/ml bFGF (C and D) or 1 ng/ml $TGF_{\beta 1}$ alone (E and F) and with neutralizing antibodies to $TGF_{\beta 1}$ (G and H). Growth factors and antibodies were added 24 h after initiation of culture, grown for a total of 7 days, and stained with rhodamine phalloidin (A, C, E, and G) and FITC labeled anti-α-SM actin (B, D, F, and H). Bar = 50 μm. Taken from Jester *et al.* (1996) with permission.

exogenous heparin derivatives (Desmouliere *et al.*, 1992b). More recently, a predominantly α-SMA expressing population have been selectively grown from sparse cultures of keratocytes (Masur *et al.*, 1996). However, when primary serum cultured keratocytes were evaluated for the expression of α-SMA, 10% of keratocytes in culture showed expression (Jester *et al.*, 1996). This finding suggested that the keratocyte activation process observed in culture also induces, partially, myofibroblast transformation based on expression of α-SMA.

Attempts to identify culture conditions that did not activate keratocytes and induce myofibroblast transformation led to the testing of various serum-free and defined culture systems. As noted above, keratocytes grown in serum containing media appeared as spindle shaped, fibroblastic-like cells (Fig. 23A). However, when primary keratocytes were isolated under serum-free conditions and cultured in the absence of serum, cells showed a dendritic phenotype, having an enlarged cell body with multiple, extending and interconnecting psuedopodia (Fig. 23B). This morphology was similar, if not identical to that observed for *in situ* keratocytes. Furthermore, cells appeared to maintain a predominantly cortical organization of actin filaments, again similar to *in situ* keratocytes (Fig. 24A). When serum-free cultured cells were stained with antibodies for α-SMA, no staining was detected (Fig. 24B), nor was protein specific for α-SMA detected on western blots. If cells were cultured in the presence of bFGF, an enlargement of the cell bodies was detected (Fig. 23C), along with an increase in the organization of actin filaments (Fig. 24C), however, no α-SMA expression was detected by immunostaining (Fig. 24D) or western blotting. By contrast, the addition of transforming growth factor beta (TGFβ) showed a marked transformation of serum-free cultured keratocytes to a fibroblastic morphology as shown by phase contrast (Fig. 23D). Additionally, TGFβ induced the formation of prominent actin filament bundles (Fig. 24E) and the expression of α-SMA as detected by both immunostaining (Fig. 24F) and western blotting. This response appeared to be specific for TGFβ since the simultaneous treatment of serum-free cultured cells with TGFβ and blocking antibodies to TGFβ inhibited both the organization of actin (Fig. 24G) and the expression of α-SMA (Fig. 24H).

These findings led to the conclusion that TGFβ was a potent inducer of myofibroblast transformation in the corneal keratocyte. Similar effects of TGFβ on α-SM actin expression and myofibroblast transformation have been shown for various cell types including bovine aortic endothelial cells (Arciniegas *et al.*, 1992), breast fibroblasts (Ronnov-Jessen and Petersen, 1993), cerebral pericytes (Verbeek *et al.*, 1994), and lens epithelium (Hales *et al.*, 1994). Based on studies showing the presence of $TGF_{\beta 1}$ specific mRNA (Wilson *et al.*, 1992; Nishida *et al.*, 1995), and protein (Nishida *et al.*, 1994; Wilson *et al.*, 1994) in both the corneal epithelium and corneal stroma, our results support both paracrine and autocrine $TGF_{\beta 1}$ response pathways involved in the induction of keratocyte transformation. Paracrine signaling by corneal epithelial cells following injury may initially lead to the recruitment of stromal keratocytes as suggested by the work of Grant et al showing that $TGF_{\beta 1}$ is a potent chemoattractant for corneal fibroblast (Grant *et al.*, 1992). Later, autocrine mechanisms may up-regulate extracellular matrix synthesis (Ohji *et al.*, 1993), down-regulate matrix degradation by inhibiting expression of matrix metalloproteinases (Girard *et al.*, 1991; Fini *et al.*, 1995), and finally initiate wound contraction by inducing the expression of α-SM actin and the transformation of stromal keratocytes to contractile myofibroblasts.

4.4. TGFβ Induced Myofibroblast Transformation in the Cornea

Since TGFβ was shown to induce myofibroblast transformation in cultured keratocytes, the obvious next question concerned the role of TGFβ in myofibroblast transformation of keratocytes in the cornea. Previous work by Shah *et al.* (1992, 1994) had demonstrated that blocking antibodies to TGFβ when administered adjacent to incisional wounds in the dermis had an inhibitory effect on scar formation. Qualitative measurements showed reductions in both monocyte and

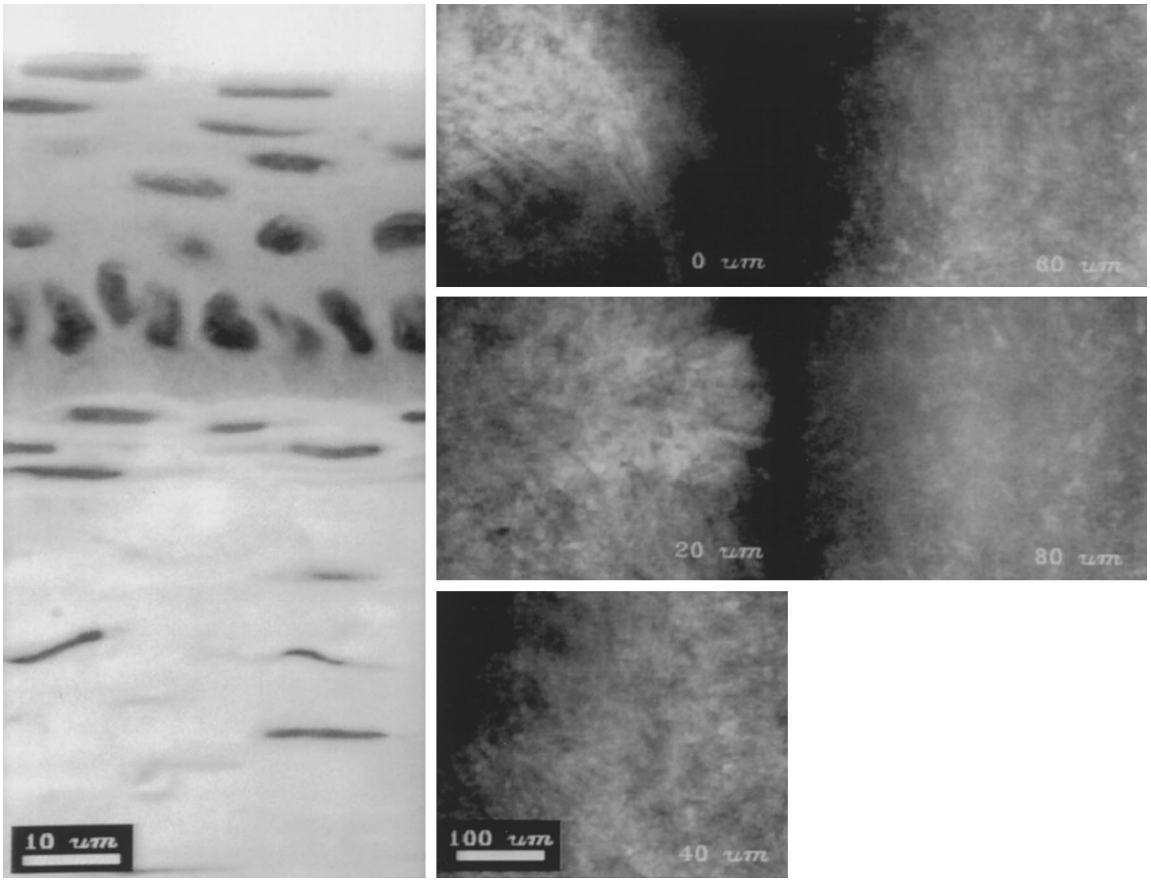

Fig. 25. Comparison of *ex vivo* light micrograph (left) with *in vivo* micrographs taken at various depths from 0 to 80 μm, 14 days after LK. Taken from Jester *et al.* (1997) with permission.

macrophage infiltration, and deposition of fibronectin, collagen type III and collagen type I following blocking of TGFβ. In studies using a similar approach, blocking monoclonal antibodies (1D11, Celrix Pharmaceuticals) that recognized TGFβ type 1–3 (Dasch *et al.*, 1989) were topically administered to rabbit corneal keratectomy wounds immediately after injury. The response of the cornea was then evaluated by confocal microscopy.

As shown previously by Tuft *et al.* (1989), keratectomy wounds in the rabbit healed by the deposition of fibrous tissue above the area of injury (Fig. 25). Using confocal microscopy, the anterior corneal fibrosis appeared as a highly reflective organization of irregularly arranged cells and extracellular matrix. Focusing through the region of fibrosis revealed a more normal appearing stromal organization consisting of regularly arranged keratocyte nuclei. The distance between the anterior, hyper-reflective region of fibrosis and the more posterior, normal stroma was used as a measure of the thickness of fibrous tissue. This thickness measured approximately 100 μm on average in untreated eyes, which significantly correlate with more conventional histologic measurements using DTAF staining ($P < 0.025$, $r = 0.627$).

Eyes that received blocking antibodies to TGFβ showed a significant reduction in the thickness of corneal fibrosis that was dose dependent (Fig. 26). In some eyes, almost no fibrosis was detected either by confocal microscopy or histologic examination. Overall, the greatest reduction in fibrosis (approximately 50% in this study) was obtained using a dose of 50 μg total protein

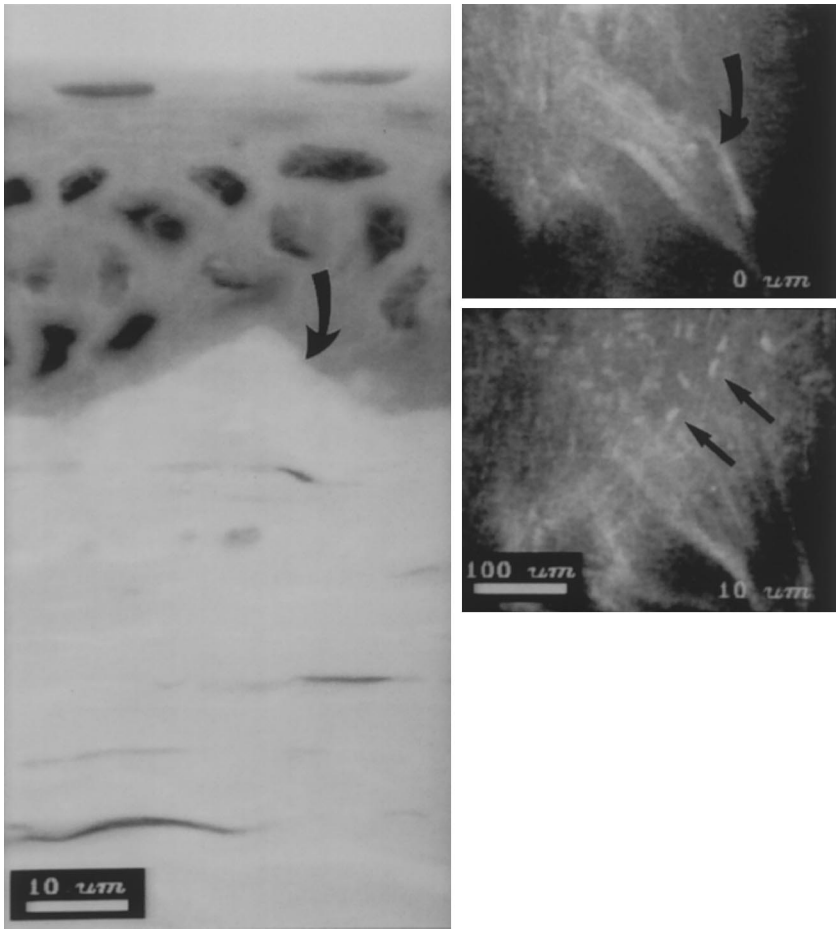

Fig. 26. Comparison of *ex vivo* light micrograph (left) with *in vivo* CM image of 14-day LK wound after treatment with 50 μg/dose 1D11. Note the presence of transected collagen lamellae at the stromal surface (arrow) and normal-appearing keratocytes immediately underneath (10 μm, small arrows). Taken from Jester *et al.* (1997) with permission.

administer 3 times a day for the first 3 days after injury. The reduction in fibrosis measured by confocal microscopy also correlated with a significant reduction ($P < 0.029$) in the deposition of fibronectin (Fig. 27) as measured by digital imaging techniques.

Overall, these findings were the first quantitative report to show that blocking antibodies to TGFβ significantly reduce corneal fibrosis *in vivo*. They were consistent with the previous work of Shah *et al.* (1992, 1994) who showed similar results for skin. What specific effect blocking antibodies have on the binding of TGFβ to keratocyte TGFβ receptors is not known, although localization studies indicated that the blocking antibodies are absorbed into the corneal stroma and may remain available to block TGFβ for a considerable length of time. Once deposited, the antibodies could block active TGFβ that is released from the corneal stroma (Nishida *et al.*, 1994) or synthesized and released by the corneal epithelium (Wilson *et al.*, 1994; Nishida *et al.*, 1995).

5. MYOFIBROBLASTS, TGF$_\beta$ AND PHOTOREFRACTIVE KERATECTOMY (PRK)

Recently, PRK using excimer laser has received increased attention for the correction of refractive errors and has essentially replaced incisional kera-

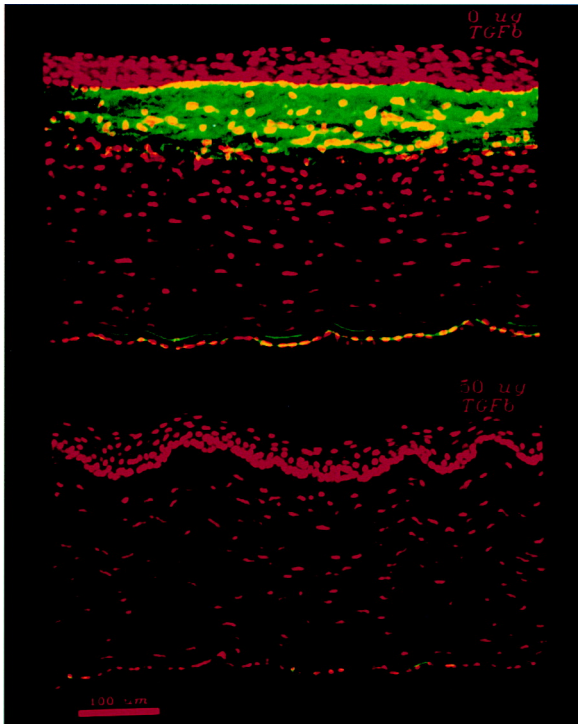

Fig. 27. Co-localization of anti-fibronectin staining (anterior corneal matrix staining) and nuclear propidium iodide staining (nuclei) in rabbit LK wounds, 56 days after treatment with 0 μg/dose (top) and 50 μg/dose 1D11 (bottom). Taken from Jester *et al.* (1997) with permission.

totomy procedures. Although current clinical results are promising, the variability, regression and post-surgical corneal "haze" have hindered the universal acceptance of this procedure (Gartry *et al.*, 1992; Brancato *et al.*, 1993; Dutt *et al.*, 1994; Sher *et al.*, 1994; Schallhorn *et al.*, 1996). Recently, clinical (Moller-Pedersen *et al.*, 1997) and experimental (Moller-Pedersen *et al.*, 1998a) studies have been undertaken by Moller-Pedersen *et al.* to identify the role of wound healing in the development of these post-operative complications. As shown for incisional keratotomy, the myofibroblast appears to be responsible for many, if not all, of the complications of this surgical procedure.

5.1. Wound Healing Following PRK

Recently published, detailed studies in rabbits using confocal microscopy have shown that PRK results in substantial keratocyte death immediately after surgery that reaches a depth of over 86 μm into the stroma. Others (Hanna *et al.*, 1989; Fantes *et al.*, 1990; Campos *et al.*, 1994) have previously identified keratocyte death following PRK; however, the extent of damage has not been previously recognized. Various mechanisms have been proposed including thermal (Tsubota *et al.*, 1993), mechanical (Kermani and Lubatschowski, 1991), and cytokine induced (Wilson *et al.*, 1996a,b). Nevertheless, following photoablation there is a characteristic and defined wound healing response. After injury, adjacent keratocytes elongate into spindle shaped cells that migrate into and re-populate over the first two weeks the remaining acellular, non-photoablated region formerly occupied by the dead keratocytes (Fig. 28A, arrows). Spindle shaped, migrating keratocytes have been previously identified using confocal microscopy by various groups (Ichijima *et al.*, 1993; Chew *et al.*, 1995).

When cellular repopulation is complete, migrating keratocytes appear to enlarge, extend pseudopodia, and become highly reflective (Fig. 28C, arrows). This morphologic phenotype appeared similar to that observed for corneal myofibroblasts as seen following incisional keratotomy (See Figs 6D, 14C and 15). The presence of myofibroblasts in PRK was then confirmed by immunocytochemistry where fibroblastic cells at the wound surface showed prominently organized actin filament bundles (Fig. 29A, B) that stain for the presence of α-SMA (Fig. 29C, D).

Brightly reflecting myofibroblasts following PRK appear to persist in the wound for the first month after surgery, showing a progressive decrease in light back scattering over time (Fig. 28E, arrows). Interestingly, Moller-Pedersen has shown that the appearance of myofibroblasts temporally correlates with a marked increase in the amount of stromal haze (Moller-Pedersen *et al.*, 1998a,b). Furthermore, the disappearance in myofibroblast reflectivity also correlates with reduced haze in the rabbit eye model. Overall, the reflectivity of the myofibroblast, appearing high at two weeks and subsiding by 2 to 3 months, temporally correlates with the previously observed haze in this animal model.

Additionally, the appearance of myofibroblasts is associated with the deposition of new collagen

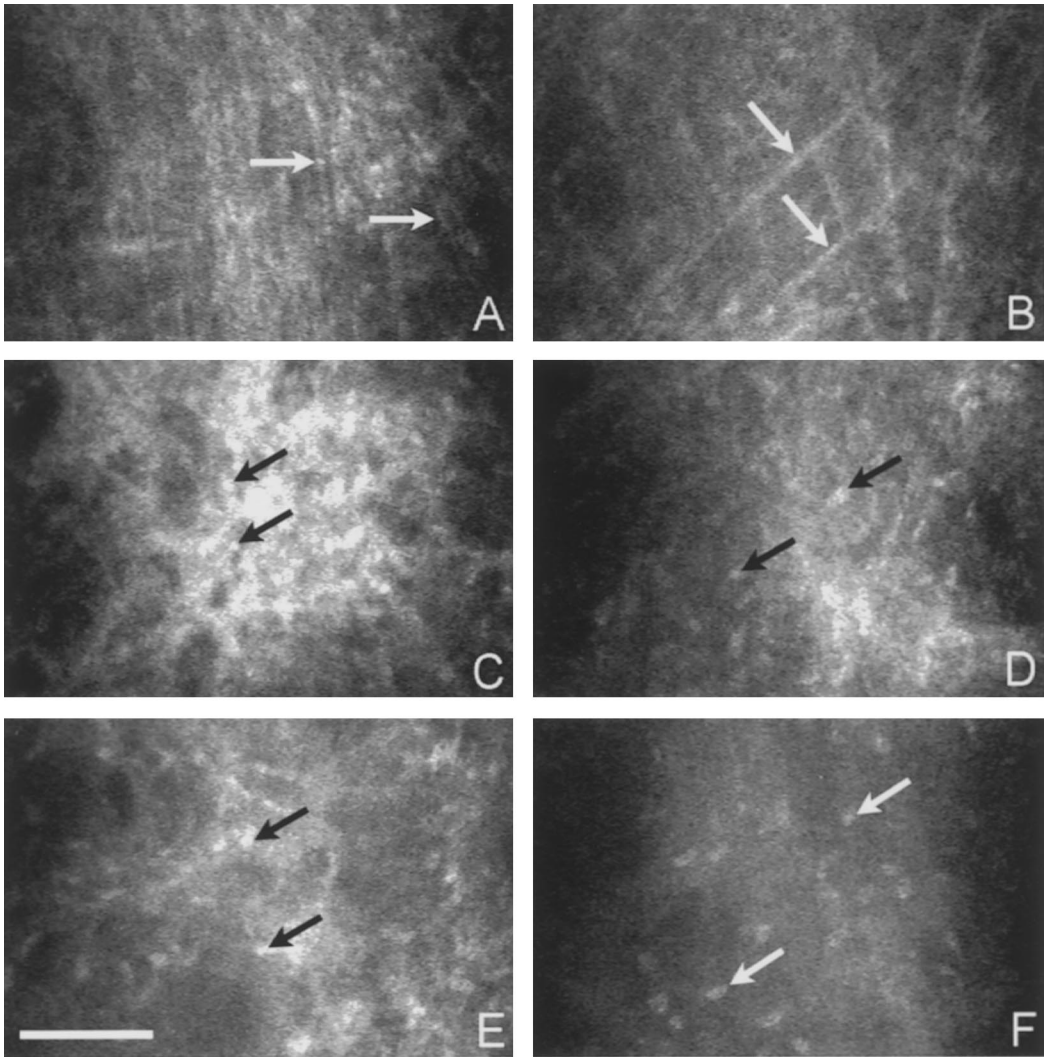

Fig. 28. *In vivo* morphology of vehicle (*left*) and anti-TGF$_\beta$ (*right*) treated rabbit corneas. *Two weeks post-PRK*: the density of repopulating, spindle-shaped keratocytes (arrows) appeared higher in vehicle treated corneas (A) than in anti-TGF$_\beta$ treated corneas (B). *Three weeks post-PRK*: the anterior stroma of vehicle treated corneas (C) had a high density of reflective, stellate cells with rounded, highly reflective nuclei (arrows), suggesting myofibroblast transformation, compared to the more normal appearing keratocytes (arrows) in anti-TGF$_\beta$ treated corneas (D). *Two months post-PRK*: cellularity (arrows) and reflectivity of the anterior stroma had decreased in both groups; however, vehicle treated corneas (E) still appeared more disorganised, hyper-cellular, and reflective compared to anti-TGF$_\beta$ treated corneas (F). Bar indicates 100 μm. Taken from Moller-Pedersen *et al.* (1998b) with permission from Oxford University Press.

tissue above the PRK photoablated stromal surface (Fig. 29A, B). The deposition of this new tissue was associated with a gradual thickening of the corneal stroma, such that by 6 months after surgery all the tissue lost by photoablation had been re-synthesized (Moller-Pedersen *et al.*, 1998a). This finding indicated that, at least for the rabbit, there is complete regression of refractive effect as measured by stromal thickness.

5.2. Role of TGF$_\beta$ in PRK

Since myofibroblasts transformation appeared to participate in post PRK wound healing and

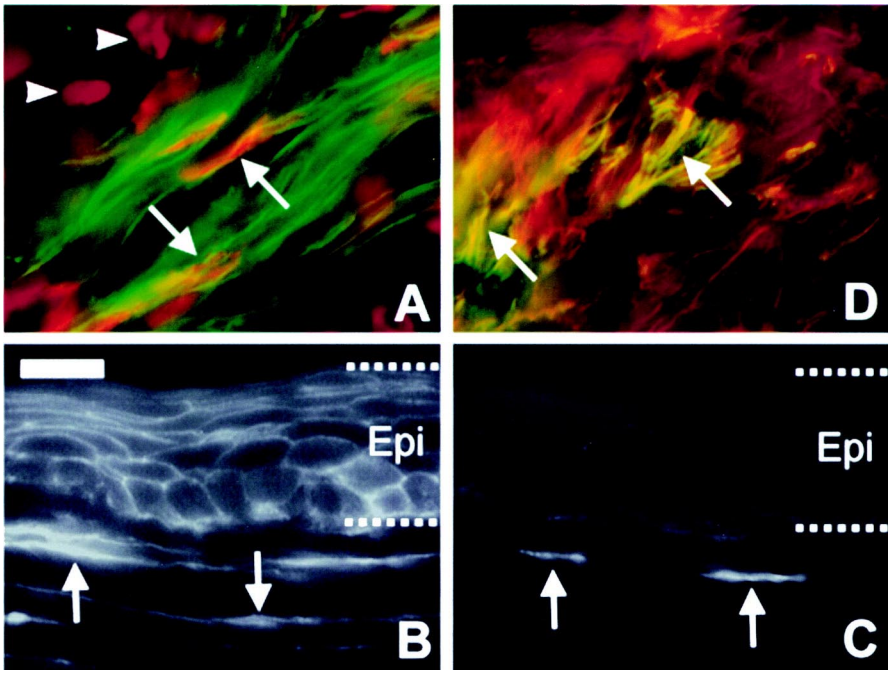

Fig. 29. Immunofluorescent staining of rabbit corneas one (A) and two-weeks (B–D) post-PRK showing expression of f-actin (stress fibers) and α-SM-actin (marker for myofibroblast transformation) within wound healing keratocytes. (A) Pseudocolored image of *en face* section showing co-localization of f-actin (green) and keratocyte nuclei (red; propidium iodide counter-staining). Note that the keratocytes appear extremely elongated and show f-actin organised into prominent microfilament bundles, i.e. stress fibers (arrows). Finally, note that adjacent cells show a weak, cortical f-actin organization (arrowheads) suggestive of quiescent keratocytes. (B) Cross-section showing intense expression of f-actin in anterior wound healing fibroblasts (arrows) as well as in the overlying epithelium (between dotted lines). (C) Same section as B showing co-localization of α-SM-actin (arrows). Only wound healing keratocytes within the photoablation zone appear to stain for both f-actin and α-SM-actin indicating myofibroblast transformation, while keratocytes below (arrowheads) did not stain for α-SM-actin (compare B and C). (D) Pseudocolored image of *en face* section showing co-localization of f-actin (red) and α-SM actin (green). Note that the cells stain intensely for α-SM actin (arrows) and have a more stellate cell morphology analogous to the *in vivo* findings. Bar indicates 25 μm. Taken from Moller-Pedersen *et al.* (1998b) with permission from Oxford University Press.

since previous studies have shown that TGFβ is a critical regulator of this transformation process, the role of TGFβ in regulating myofibroblast transformation following PRK was evaluated (Moller-Pedersen *et al.*, 1998b). Following PRK, rabbits eyes were treated topically with 50 μg of blocking antibody (mouse monoclonal 1D11), three times a day for 3 days. Within the first week after surgery, anti-TGFβ treated eyes showed a marked decrease in the apparent number of spindle shaped, migratory keratocytes compared to untreated controls (Fig. 28B, arrows). This decrease could be attributed to both inhibition of TGFβ's chemotactic (Grant *et al.*, 1992) and growth up-regulatory (Ohji *et al.*, 1993; Jester *et al.*, 1996) effects. Most remarkable was the observation that after repopulation of the acellular stroma fewer cells appeared to become hyperreflective (Fig. 28D, arrows) and those that did showed a more rapid loss and return to a normal keratocyte reflectivity (Fig. 28F, arrows). Furthermore, corneal "haze" following treatment was significantly reduced both in extent (peak haze) and duration (time to return to baseline).

Overall, these observations support the conclusion that TGFβ plays an important role in controlling myofibroblast transformation following PRK and that blocking antibodies to TGFβ can inhibit this transformation process. Unfortunately, it was not possible to confirm the absence of myofibroblasts in treated eyes since treatment with 1D11 interferes with immunocytochemical localization using mouse monoclonal antibodies. Furthermore, TGFβ mediated myofi-

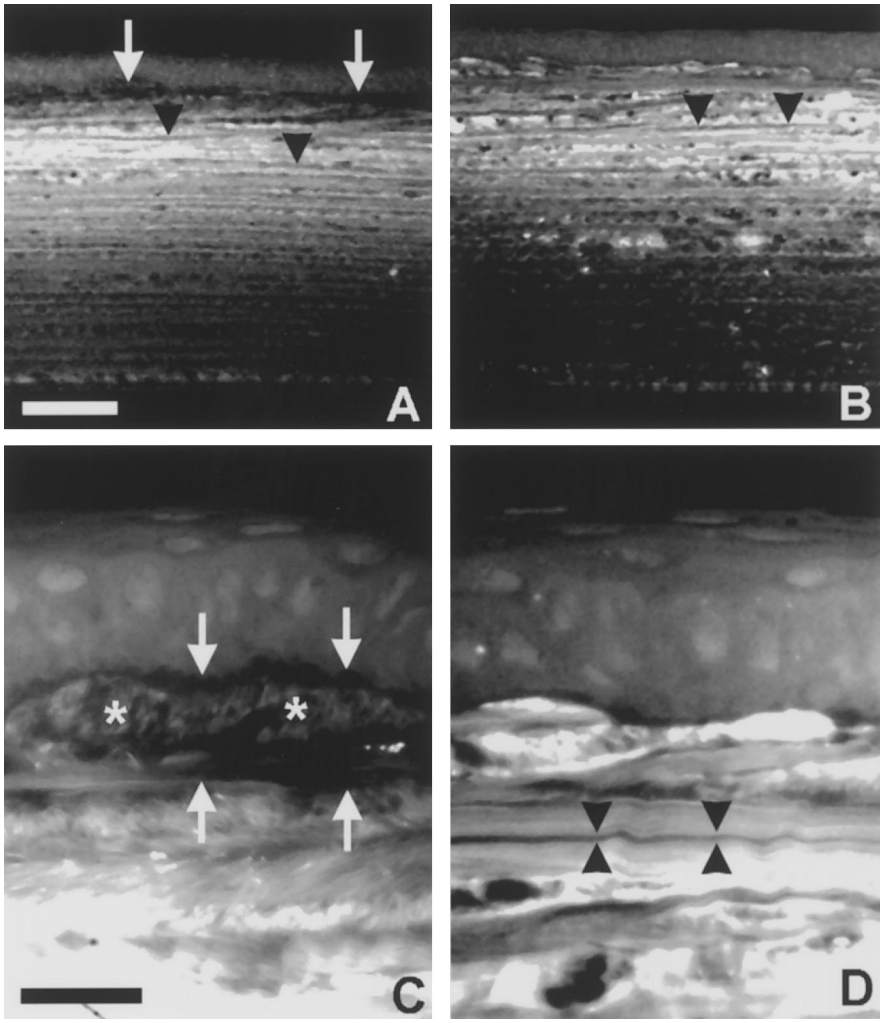

Fig. 30. Fluorescence microscopy of DTAF-stained corneas four months post-PRK. In both vehicle (A,C) and anti-TGF$_\beta$ (B,D) treated corneas, the anterior stroma contained fluorescently stained lamellae, whereas the posterior stroma was unstained. In vehicle treated cornea (A,C), there was a non-fluorescent subepithelial band (20–25 μm; corrected for shrinkage) (arrows) indicating deposition of new, fibrotic extracellular matrix *above* the photoablated stromal surface (defined as stromal *fibrosis*). Note the extension of fluorescently stained lamellae (asterisks) into the area of fibrosis (C). In contrast, no unstained subepithelial zone was observed in anti-TGF$_\beta$ treated cornea (B,D). In both vehicle and anti-TGF$_\beta$ treated corneas, very thin (<2 μm), non-fluorescent lamellae (arrowheads) were interwoven with fluorescently stained lamellae (A, B, C), suggesting stromal *regeneration* (growth *below* the photoablated stromal surface). White bar indicates 100 μm in A, B. Black bar indicates 20 μm in C, D. Taken from Moller-Pedersen *et al.* (1998b) with permission from Oxford University Press.

broblast transformation appears to play an important role in the development of corneal "haze" after PRK. Although recent studies have suggested that apoptosis and initial keratocyte death may be important regulators of the development of corneal "haze" and wound healing (Helena *et al.*, 1998), most of the changes observed following PRK, i.e. cell migration, growth up-regulation, myofibroblast proliferation, appear to be regulated by TGFβ. Clearly, further study is necessary to clarify the exact role of apoptosis in this process.

In addition to the effects of myofibroblasts on corneal "haze", blocking antibodies to TGFβ also substantially reduce or abolished the deposition of new extracellular matrix above the

photoablated stroma (Fig. 30B, D). Since TGFβ up-regulates matrix synthesis this effect was expected, and may, in part, explain the decreased corneal "haze" following antibody treatment. However, detailed measurements by Moller-Pedersen failed to show any effect of anti-TGFβ treatment on the progressive growth of the corneal stroma after photoablation in the rabbit (Moller-Pedersen *et al.*, 1998b). With the absence of fibrosis, there is no known explanation for this growth other than by normal stromal mechanisms that appear to be TGFβ-independent.

Overall, therefore, the findings that have recently been published strongly implicate wound healing, and, more specifically, myofibroblast transformation as the cause of two major complications associated with PRK. First, the presence of myofibroblasts within the wound bed causes a marked increase in back scattering from the cornea that is seen clinically as corneal "haze". Second, the appearance of myofibroblasts in the wound initiates the deposition of fibrous tissue that leads, in part, to thickening of the corneal stroma and regression of the refractive effect. These studies also demonstrate that the control of these cells by the use of blocking antibodies to TGFβ significantly reduces the presence of myofibroblasts and eliminates at least one complication, corneal "haze".

Extension of these findings in the rabbit to the clinical results following PRK in man, is, of course, problematical. However, lessons from incisional keratotomy indicate that for some patients, healing of human PRK may require years to decades to accomplish, if it occurs at all. In those patients which develop a normal healing response, we may expect to see substantial regression with haze. Time will ultimately tell us the consequences of failed wound healing in those patients who do not regress. Finally, the finding that the cornea of the rabbit returns to its pre-operative thickness is remarkable and suggests a previously unrecognized, dynamic mechanism controlling corneal growth and curvature throughout life. We can only speculate on the consequences of such a mechanism in the human, and its meaning to any form of current or future refractive surgery.

6. FUTURE DIRECTIONS

This review has presented evidence that implicates the corneal keratocyte and the process of keratocyte transformation to a myofibroblast phenotype as playing a pivotal role in determining the outcome of refractive surgery. Although myofibroblasts appear to lie at the heart of the variable and unpredictable nature of refractive surgery, four basic questions remain concerning the process of transformation, wound contraction, corneal "haze" and regression. First, and of primary interest, is the elucidation of the cellular and molecular events governing myofibroblast transformation of the keratocyte. While studies have already identified TGFβ as playing an important role, the molecular mechanisms by which quiescent keratocytes develop a contractile function have yet to be demonstrated. The unique and very finitely localized environment in which myofibroblast transformation takes place suggests that growth factors such as TGFβ do not act alone but that environmental signals are important. These signals might include the matrix that is deposited by the keratocyte or interaction between the cells themselves. Our laboratory has recently focused on the generation of mechanical signals provided by the extracellular matrix and their potential control of contractile protein expression and organization. Integrins receptors have been shown to provide an "*outside-in*", mechotransduction signaling pathway (Wang *et al.*, 1993; Wang and Ingber, 1994) that regulates cell shape and gene expression. What signals are transmitted to the keratocyte in different matrix environments is not known. How integrin-signaling pathways combine and interact with growth factor signaling in myofibroblast transformation is not clear. In addition to the matrix, myofibroblasts clearly remain interconnected, forming an interwoven network within the wound volume. Work by Masur *et al.* (1996) and others (i.e., Petridou and Masur, 1996) suggest important changes in cell–cell attachment proteins, cadherins and catenins, may modulate and control these interconnection, while controlling the process of myofibroblast transformation. What regulates cell–cell connections in the wound and how cell–cell interactions participate in wound contraction

are important questions that are only now beginning to be addressed.

Second, though wound healing studies implicate a muscle-like contractile process in the generation of the mechanical tension necessary to close wounds, what generates this force remains controversial. Past work using cell culture models has implicated cellular locomotion in the generation of intracellular forces that are transmitted to the underlying matrix leading to matrix distortion and organization (Harris *et al.*, 1980). More recently, however, studies using an *in vitro* force measurement assay have questioned this model (Roy *et al.*, 1998). Although keratocytes exert force on a collagen matrix the process of cell translocation dissipates these forces leading to no net change in the organization of matrix. If cells exert force through a motility based mechanism, *a paradox then arises where cells must migrate to exert force but not migrate to reorganize the matrix*. Clearly, the continued study of mechanical force generation of cells on relevant extracellular matrices is needed to resolve this seminal issue.

Third, while the appearance of myofibroblasts in PRK is related to the development of corneal "haze", the cause for haze is still unknown. Most studies have focused on the role of the extracellular matrix in controlling corneal transparency and opacification after injury. However, studies using confocal microscopy to detect the back scattering and reflecting structures with in the eye show a *cellular-based* pattern to transparency that has previously not been recognized. In the corneal epithelium, the high expression of two water soluble proteins, transketolase (TKT) and aldehyde dehydrogenase class 3 (ALDH3) has been proposed as playing a role in control the cellular transparency of the epithelium (Sax *et al.*, 1996; Kays and Piatigorsky, 1997). Whether a similar mechanism is present in the keratocytes is currently under study in our laboratory.

Finally, the continued growth of the cornea following treatment of PRK with antibodies to TGFβ is a perplexing and unexpected finding. Fundamentally, this growth suggests that the thickness and hence curvature is dynamically regulated by an unknown mechanism that is independent of TGFβ. What is controlling corneal growth has important implications in many corneal diseases including refractive errors, astigmatism, and keratoconus. Clearly an important direction for future work is identifying the mechanisms underlying potential maintenance of a "normal" corneal thickness.

Acknowledgements—Acknowledgement is extended to those collaborators and mentors who have given so much of their time, effort and resources to the completion of this body of work and for whom authorship on this paper could not be accommodated. Special recognition is extended to Ronald E. Smith and Meryln Rodrigues in whose laboratories the early investigations were carried out and to Mojmir Petran and Michael Lemp for first introducing me to confocal microscopy. Additionally, we are all indebted to the tireless and patient work of Torben Moller-Pedersen who has spent many long hours analyzing confocal images of PRK and to Patricia Barry-Lane for whom no task was impossble. We would like further to recognize the National Eye Institute (EY07438) and Research to Prevent Blindness, Inc (unrestricted grants, Senior Scientist Awards, and Manpower Awards) whose funding support has made this work possible. Finally, this work is dedicated to the corneal keratocyte that is like the grain of sand to the oyster, a mere irritation to some, but a wonder of nature to those who take time to look.

REFERENCES

Abercrombie, M., Flint, M. H. and James, D. W. (1956) Wound contraction in relation to collagen formation in scorbutic guinea-pigs. *J. Embryol. Exp. Med.* **4,** 167–175.

Abercrombie, M., James, D. W. and Newcombe, J. F. (1960) Wound contraction in rabbit skin, studied by splinting the wound margins. *J. Anat.* **94,** 170–182.

Akiyama, S. K., Yamada, S. S., Chen, W.-T. and Yamada, K. M. (1989) Analysis of fibronectin receptor function with monoclonal antibodies: roles in cell adhesion, migration, matrix assembly and cytoskeletal organization. *J. Cell Biol.* **109,** 863–875.

Arciniegas, E., Sutton, A. B., Allen, T. D. and Shor, A. M. (1992) Transforming growth factor beta 1 promotes the differentiation of endothelial cells into smooth muscle-like cells *in vitro*. *J. Cell Sci.* **103,** 521–529.

Beyer, E. C., Kistler, J., Paul, D. L. and Goodenough, D. A. (1989) Antisera directed against connexin 43 peptides react with a 43-kD protein localized to gap junctions in myocardium and other tissues. *J. Cell Biol.* **108,** 595–605.

Binder, P. S., Nayak, S. K., Deg, J. K., Zavala, E. Y. and Sugar, J. (1987) Ultrastructural and histochemical study of long-term wound healing after radial keratotomy. *Am. J. Ophthalmol.* **103,** 432–440.

Brancato, R., Travola, A. and Carones, F. *et al.* (1993) Excimer laser photorefractive keratectomy for myopia: results in 1165 eyes. Italian study group. *Refract. Corneal Surg.* **9,** 95–104.

Campos, M., Raman, S., Lee, M. and McDonnell, P. J. (1994) Keratocyte loss after different methods of de-epithelialization. *Ophthalmology* **101,** 890–894.

Cavanagh, H. D., Petroll, W. M. and Jester, J. V. (1995) Confocal microscopy: uses in measurement of cellular structure and function. *Progress in Retinal and Eye Research* **14,** 527–565.

Chew, S. J., Beuerman, R. W., Kaufman, H. E. and McDonald, M. B. (1995) *In vivo* confocal microscopy of corneal wound healing after excimer laser photorefractive keratectomy. *CLAO Journal* **21,** 273–280.

Cintron, C., Hassinger, L. C., Kublin, C. L. and Cannon, D. J. (1978) Biochemical and ultrastructural changes in collagen during corneal wound healing. *J. Ultrastruct. Res.* **65,** 13–22.

Cintron, C., Schneider, H. and Kublin, C. (1973) Corneal scar formation. *Exp. Eye Res.* **17,** 251–259.

Cintron, C., Szamier, R. B., Hassinger, L. C. and Kublin, C. L. (1982) Scanning electron microscopy of rabbit corneal scars. *Invest. Ophthalmol. Vis. Sci.* **23,** 50–63.

Darby, I., Skalli, O. and Gabbiani, G. (1990) Alpha-smooth muscle actin is transiently expressed by myofibroblasts during experimental wound healing. *Lab. Invest.* **63,** 21–29.

Dasch, J. R., Pace, D. R., Waegell, W., Inenaga, D. and Ellingsworth, L. (1989) Monoclonal antibodies recognizing transforming growth factor-beta. Bioactivity neutralization and transforming growth factor beta 2 affinity purification. *J. Immunol.* **142,** 1536–1541.

Deg, J. K., Zavala, E. Y. and Binder, P. S. (1985) Delayed corneal wound healing following radial keratotomy. *Ophthalmol.* **92,** 734–740.

Desmouliere, A., Geinoz, A., Gabbiani, F. and Gabbiani, G. (1993) Transforming growth factor-beta 1 induces alpha-smooth muscle actin expression in granulation tissue myofibroblasts and in quiescent and growing cultured fibroblasts. *J. Cell Biol.* **122,** 103–111.

Desmouliere, A., Rubbia-Brandt, L., Abdiu, A., Walz, T., Macieira-Coelho, A. and Gabbiani, G. (1992a) Alpha-smooth muscle actin is expressed in a subpopulation of cultured and cloned fibroblasts and is modulated by gamma-interferon. *Exp. Cell Res.* **201,** 64–73.

Desmouliere, A., Rubbia-Brandt, L., Grau, G. and Gabbiani, G. (1992b) Heparin induces alpha-smooth muscle actin expression in cultured fibroblasts and in granulation tissue myofibroblasts. *Lab. Invest.* **67,** 716–726.

Dutt, S., Steinert, R. F., Raizman, M. B. and Puliafito, C. A. (1994) One-year results of excimer laser photorefractive keratectomy for low to moderate myopia. *Arch. Ophthalmol.* **112,** 1427–1436.

Fantes, F. E., Hanna, K. D., Waring, G. O.d., Pouliquen, Y., Thompson, K. P. and Savoldelli, M. (1990) Wound healing after excimer laser keratomileusis (photorefractive keratectomy) in monkeys [see comments]. *Arch. Ophthalmol.* **108,** 665–675.

Fini, M. E., Girard, M. T., Matsubara, M. and Bartlett, J. D. (1995) Unique regulation of the matrix metalloproteinase, gelatinase B. *Invest. Ophthalmol. Vis. Sci.* **36,** 622–633.

Fyodorov, S. N. and Durnev, V. V. (1979) Operation of dosage dissection of corneal circular ligament in cases of myopia of mild degree. *Ann. Ophthalmol.* **11,** 1885–1890.

Fyodorov, S. N. and Durnev, V. V. (1981) Surgical correction of complicated myopic astigmatism by means of dissection of circular ligament of cornea. *Ann. Ophthalmol.* **13,** 115.

Gabbiani, G., Chaponnier, C. and Huttner, I. (1978) Cytoplasmic filaments and gap junctions in epithelial cells and myofibroblasts during wound healing. *J. Cell Biol.* **76,** 561–568.

Gabbiani, G., Hirschel, B. J., Ryan, G. B., Statkov, P. R. and Majno, G. (1972) Granulation tissue as a contractile organ. A study of structure and function. *J. Exp. Med.* **135,** 719–734.

Gabbiani, G., Ryan, G. B. and Majno, G. (1971) Presence of modified fibroblasts in granulation tissue and their possible role in wound contraction. *Experientia* **27,** 549–550.

Garana, R. M., Petroll, W. M., Chen, W. T., Herman, I. M., Barry, P., Andrews, P., Cavanagh, H. D. and Jester, J. V. (1992) Radial keratotomy. II. Role of the myofibroblast in corneal wound contraction. *Invest. Ophthalmol. Vis. Sci.* **33,** 3271–3282.

Gartry, D. S., Kerr Muir, M. G. and Marshall, J. (1992) Excimer laser photorefractive keratectomy. 18-month follow-up. *Ophthalmology* **99,** 1209–1219.

Girard, M. T., Matsubara, M. and Fini, M. E. (1991) Transforming growth factor-beta and interleukin-1 modulate metalloproteinase expression by corneal stromal cells. *Invest. Ophthalmol. Vis. Sci.* **32,** 2441–2454.

Glasgow, B. J., Brown, H. H., Aizuss, D. H., Mondino, B. J. and Foos, R. Y. (1988) Traumatic dehiscence of incisions seven years after radial keratotomy. *Am. J. Ophthalmol.* **106,** 703–707.

Grant, M. B., Khaw, P. T., Schultz, G. S., Adams, J. L. and Shimizu, R. W. (1992) Effects of epidermal growth factor, fibroblast growth factor and transforming growth factor-beta on corneal cell chemotaxis. *Invest. Ophthalmol. Vis. Sci.* **33,** 3292–3301.

Gressner, A. M. (1991) Liver fibrosis, perspectives in pathobiochemical research and clinical outlook. *Eur. J. Clin. Chem. Clin. Biochem.* **29,** 293–311.

Hales, A. M., Schulz, M. W., Chamberlain, C. G. and McAvoy, J. W. (1994) TGF-beta 1 induces lens cells to accumulate alpha-smooth muscle actin, a marker for subcapsular cataracts. *Curr. Eye Res.* **13,** 885–890.

Hanna, K. D., Pouliquen, Y. M. and Waring, G. O. *et al.* (1989) Corneal stromal wound healing in rabbits after 193-nm excimer laser surface ablation. *Arch. Ophthalmol.* **107,** 895–901.

Harris, A. K., Wild, P. and Stopak, D. (1980) Silicone rubber substrata: a new wrinkle in the study of cell locomotion. *Science* **208,** 177–189.

Hasty, D. L. and Hay, E. D. (1977) Freeze-fracture studies of the developing cell surface, I: The plasmalemma of the corneal fibroblast. *J. Cell Biol.* **72,** 667–686.

Hay, E. D. (1980) Development of vertebrate cornea. *Int. Rev. Cytol.* **63,** 263–322.

Helena, M. C., Baerveldt, F., Kim, W.-J. and Wilson, S. E. (1998) Keratocyte apoptosis after corneal surgery. *Invest. Ophthalmol. Vis. Sci.* **39,** 276–283.

Ichijima, H., Petroll, W. M., Jester, J. V., Barry, P. A., Andrews, P. M., Dai, M. and Cavanagh, H. D. (1993) *In vivo* confocal microscopic studies of endothelial wound healing in rabbit cornea. *Cornea* **12,** 369–378.

Ishizaki, M., Zhu, G., Haseba, T., Shafer, S. S. and Kao, W. W.-Y. (1994) Expression of collagen I, smooth muscle alpha-actin and vimentin during the healing of alkali-

burned and lacerated corneas. *Invest. Ophthalmol. Vis. Sci.* **34,** 3320–3328.

Jester, J. V., Barry, P. A., Lind, G. J., Petroll, W. M., Garana, R. and Cavanagh, H. D. (1994) Corneal keratocytes: *in situ* and *in vitro* organization of cytoskeletal contractile proteins. *Invest. Ophthalmol. Vis. Sci.* **35,** 730–743.

Jester, J. V., Barry-Lane, P. A., Cavanagh, H. D. and Petroll, W. M. (1996) Induction of alpha-smooth muscle actin expression and myofibroblast transformation in cultured corneal keratocytes. *Cornea* **15,** 505–516.

Jester, J. V., Barry-Lane, P. A., Petroll, W. M., Olsen, D. R. and Cavanagh, H. D. (1997) Inhibition of corneal fibrosis by topical application of blocking antibodies to TGFbeta in the rabbit. *Cornea* **16,** 177–187.

Jester, J. V., Petroll, W. M., Barry, P. A. and Cavanagh, H. D. (1995) Temporal, 3-dimensional, cellular anatomy of corneal wound tissue. *J. Anat.* **186,** 301–311.

Jester, J. V., Petroll, W. M., Feng, W., Essepian, J. and Cavanagh, H. D. (1992b) Radial keratotomy. 1. The wound healing process and measurement of incisional gape in two animal models using *in vivo* confocal microscopy. *Invest. Ophthalmol. Vis. Sci.* **33,** 3255–3270.

Jester, J. V., Petroll, W. M., Garana, R. M., Lemp, M. A. and Cavanagh, H. D. (1992a) Comparison of *in vivo* and *ex vivo* cellular structure in rabbit eyes detected by tandem scanning microscopy. *J. Micros.* **165,** 169–181.

Jester, J. V., Rodrigues, M. M. and Herman, I. M. (1987) Characterization of avascular corneal wound healing fibroblasts. New insights into the myofibroblast. *Am. J. Pathol.* **127,** 140–148.

Jester, J. V., Steel, D., Salz, J., Miyashiro, J., Rife, L., Schanzlin, D. J. and Smith, R. E. (1981) Radial keratotomy in non-human primate eyes. *Am. J. Ophthalmol.* **92,** 153–171.

Jester, J. V., Villasenor, R. A. and Miyashiro, J. (1983) Epithelial inclusion cysts following radial keratotomy. *Arch. Ophthalmol.* **101,** 611–615.

Jester, J. V., Villasenor, R. A., Schanzlin, D. J. and Cavanagh, H. D. (1992c) Variations in corneal wound healing after radial keratotomy: possible insights into mechanisms of clinical complications and refractive effects. *Cornea* **11,** 191–199.

Johnson, R. J., Floege, J., Yoshimura, A., Iida, H., Couser, W. G. and Alpers, C. E. (1992) The activated mesangial cell, a glomerular 'myofibroblast'? *J. Am. Soc. Nephrol.* **2,** S190–S197.

Kaye, G. I. (1969) Stereologic measurement of cell volume fraction of rabbit corneal stroma. *Arch. Ophthalmol.* **82,** 792–794.

Kays, W. T. and Piatigorsky, J. (1997) Aldehyde dehydrogenase class 3 expression: identification of a cornea-preferred gene promoter in transgenic mice. *Proc. Natl. Acad. Sci.* **94,** 13594–13599.

Kermani, O. and Lubatschowski, H. (1991) Structure and dynamics of photo-acoustic shock-waves in 193 nm excimer laser photoablation of the cornea. *Fortshr. Ophthalmol.* **88,** 748–753.

Knauss, W., Rapacz, P. and Sene, K. (1981) Curvature changes induced by radial keratotomy in solithane model of eye. *Invest. Ophthalmol. Vis. Sci.* **20**(Suppl), 69.

Kokott, W. (1938) Uber mechanisch-funktionelle strukturen des auges. *Arch. Ophthalmol.* **138,** 424–485.

Kuwabara, T., Perkins, D. G. and Cogan, D. G. (1976) Sliding of the epithelium in experimental corneal wounds. *Invest. Ophthalmol. Vis. Sci.* **15,** 4–14.

Lemp, M. A., Dilly, P. N. and Boyde, A. (1986) Tandem scanning (confocal) microscopy of the full thickness cornea. *Cornea* **4,** 205–209.

Luttrull, J. K., Smith, R. E. and Jester, J. V. (1985) *In vitro* contractility of avascular corneal wounds in rabbit eyes. *Invest. Ophthalmol. Vis. Sci.* **26,** 1449–1452.

Majno, G., Gabbiani, G., Hirschel, B. J., Ryan, G. B. and Statkov, P. R. (1971) Contraction of granulation tissue *in vitro*: similarity to smooth muscle. *Science* **173,** 548–550.

Masur, S. K., Cheung, J. K. H. and Antohi, S. (1993) Identification of integrins in cultured corneal fibroblasts and in isolated keratocytes. *Invest. Ophthalmol. Vis. Sci.* **34,** 2690–2698.

Masur, S. K., Dewal, H. S., Dinh, T. T., Erenburg, I. and Petridou, S. (1996) Myofibroblasts differentiate from fibroblasts when plated at low density. *Proc. Natl. Acad. Sci. USA* **93,** 4219–4223.

Matsuda, H. and Smelser, G. K. (1973) Electron microscopy of corneal wound healing. *Exp. Eye Res.* **16,** 427–442.

Maurice, D. M. (1957) The structure and transparency of the cornea. *J. Physiol.* **136,** 263–286.

Maurice, D. M. (1962) The Cornea and Sclera. In *The Eye*, Vol. 1 (Ed. H. Davson) pp. 289–361. Academic Press, New York.

Moller-Pedersen, T., Li, H. F., Petroll, W. M., Cavanagh, H. D. and Jester, J. V. (1998a) Confocal microscopic characterization of wound repair after photorefractive keratectomy. *Invest. Ophthalmol. Vis. Sci.* **39,** 487–501.

Moller-Pedersen, T., Cavanagh, H. D., Petroll, W. M. and Jester, J. V. (1998b) Neutralizing antibody to TGFbeta modulates stromal fibrosis but not regression of photoablative effect following PRK. *Curr. Eye Res.* **17,** 736–747.

Moller-Pedersen, T., Vogel, M., Li, H. F., Petroll, W. M., Cavanagh, H. D. and Jester, J. V. (1997) Quantification of stromal thinning, epithelial thickness and corneal haze after photorefractive keratectomy using *in vivo* confocal microscopy. *Ophthalmology* **104,** 360–368.

Muller, L. J., Pels, L. and Vrensen, G. F. J. M. (1995) Novel aspects of the ultrastructural organization of human corneal keratocytes. *Invest. Ophthalmol. Vis. Sci.* **36,** 2557–2567.

Nishida, K., Kinoshita, S., Yokoi, N., Kaneda, M., Hashimoto, K. and Yamamoto, S. (1994) Immunohistochemical localization of transforming growth factor-beta 1, -beta 2 and -beta 3 latency-associated peptide in human cornea. *Invest. Ophthalmol. Vis. Sci.* **35,** 3289–3294.

Nishida, K., Sotozono, C., Adachi, W., Yamamoto, S., Yokoi, N. and Kinoshita, S. (1995) Transforming growth factor-beta 1, -beta 2 and -beta 3 mRNA expression in human cornea. *Curr. Eye Res.* **14,** 235–241.

Nishida, T., Yasumoto, K., Otori, T. and Desaki, J. (1988) The network structure of corneal fibroblasts in the rat as revealed by scanning electron microscopy. *Invest. Ophthalmol. Vis. Sci.* **29,** 1887–1890.

Ohji, M., SundarRaj, N. and Thoft, R. A. (1993) Transforming growth factor-beta stimulates collagen and fibronectin synthesis by human corneal stromal fibroblasts *in vitro*. *Current Eye Research* **12,** 703–709.

Petridou, S. and Masur, S. K. (1996) Immunodetection of connexins and cadherins in corneal fibroblasts and myofibroblasts. *Invest. Ophthalmol. Vis. Sci.* **37,** 1740–1748.

Petroll, W. M., Boettcher, K., Barry, P., Cavanagh, H. D. and Jester, J. V. (1995) Quantitative assessment of anteroposterior keratocyte density in the normal rabbit cornea. *Cornea* **14,** 3–9.

Petroll, W. M., Cavanagh, H. D., Barry, P., Andrews, P. and Jester, J. V. (1993a) Quantitative analysis of stress fiber orientation during corneal wound contraction. *J. Cell Sci.* **104,** 353–363.

Petroll, W. M., Cavanagh, H. D. and Jester, J. V. (1993b) Three-dimensional imaging of corneal cells using *in vivo* confocal microscopy. *J. Micros.* **170,** 213–219.

Petroll, W. M., Cavanagh, H. D., Lemp, M. A., Andrews, P. M. and Jester, J. V. (1992a) Digital image acquisition in *in vivo* confocal microscopy. *J. Micros.* **165,** 61–69.

Petroll, W. M., New, K., Sachdev, M., Cavanagh, H. D. and Jester, J. V. (1992b) Radial keratotomy. III. Relationship between wound gape and corneal curvature in primate eyes. *Invest. Ophthalmol. Vis. Sci.* **33,** 3283–3291.

Puliafito, C. A., Wong, K. and Steinert, R. F. (1987) Quantitative and ultrastructural studies of excimer laser ablation of the cornea at 193 and 248 nanometers. *Las. Surg. Med.* **7,** 155–159.

Ronnov-Jessen, L. and Petersen, O. W. (1993) Induction of alpha-smooth muscle actin by transforming growth factor-beta1 in quiescent human breast gland fibroblasts. *Lab. Invest.* **68,** 696–707.

Roy, P., Petroll, W. M., Cavanagh, H. D., Chuong, C. J. and Jester, J. V. (1998) An *in vitro* force measurement assay to study the early mechanical interaction between corneal fibroblasts and collagen matrix. *Exp. Cell Res.* **232,** 106–117.

Sato, T., Akiyama, K. and Shibata, H. (1953) A new surgical approach to myopia. *Am. J. Ophthalmol.* **36,** 823–829.

Sax, C. M., Salamon, C., Kays, W. T., Guo, J., Yu, F., Cuthbertson, R. A. and Piatigorsky, J. (1996) Transketolase is a major protein in the mouse cornea. *J. Biol. Chem.* **271,** 33568–33574.

Schachar, R. A., Black, T. D. and Huang, T. (1981) Understanding radial keratotomy. LAL Publishing, Denison, Texas. 12–37, 79–99.

Schachar, R. A., Levy, N. S. and Schachar, L. (1980). Radial keratotomy. LAL Publishing, Denison, Texas.

Schallhorn, S. C., Blanton, C. L., Kaupp, S. E., Sutphin, J., Gordon, M., Goforth, H., Jr and Butler, F. K., Jr (1996) Preliminary results of photorefractive keratectomy in active-duty United States Navy personnel. *Ophthalmology* **103,** 5–22.

Shah, M., Foreman, D. M. and Ferguson, M. W. (1992) Control of scarring in adult wounds by neutralising antibody to transforming growth factor beta. *Lancet* **339,** 213–214.

Shah, M., Foreman, D. M. and Ferguson, M. W. (1994) Neutralising antibody to TGF-beta 1,2 reduces cutaneous scarring in adult rodents. *J. Cell Sci.* **107,** 1137–1157.

Sher, N. A., Hardten, D. R. and Fundingsland, B. *et al.* (1994) 193-nm excimer photorefractive keratectomy in high myopia. *Ophthalmology* **101,** 1575–1582.

Skalli, O., Ropraz, P., Trzeciak, A., Benzonana, G., Gillessen, D. and Gabbiani, G. (1986) A monoclonal antibody against alpha-smooth muscle actin: a new probe for smooth muscle differentiation. *J. Cell Biol.* **103,** 2787–2796.

Tanaka, M., Ishii, R., Yamaguchi, T., Kanai, A. and Nakajima, A. (1980) Bullous keratopathy after the operation for myopia. *Acta Soc. Ophthalmol. Japan* **84,** 2068–2074.

Trokel, S. (1989) Evolution of excimer laser corneal surgery [see comments]. *J. Cat. Ref. Surg.* **15,** 373–383.

Tsubota, K., Toda, I. and Itoh, S. (1993) Reduction of subepithelial haze after photorefractive keratectomy by cooling the cornea [letter]. *Am. J. Ophthalmol.* **115,** 820–821.

Tuft, S. J., Zabel, R. W. and Marshall, J. (1989) Corneal repair following keratectomy. A comparison between conventional surgery and laser photoablation. *Invest. Ophthalmol. Vis. Sci.* **30,** 1769–1777.

Ueda, A., Nishida, T., Otori, T. and Fujita, H. (1987) Electron-microscopic studies on the presence of gap junctions between corneal fibroblasts in rabbits. *Cell Tiss. Res.* **249,** 473–479.

Ussmann, J. H., Lazarides, E. and Ryan, S. J. (1980) Traction retinal detachment: a cell-mediated event. *Arch. Ophthalmol.* **99,** 869.

Verbeek, M. M., Otte-Holler, I., Wesseling, P., Ruiter, D. J. and de Waal, R. M. (1994) Induction of alpha-smooth muscle actin expression in cultured human brain pericytes by transforming growth factor-beta 1. *Am. J. Pathol.* **144,** 372–382.

Wang, N., Butler, J. P. and Ingber, D. E. (1993) Mechanotransduction across the cell surface and through the cytoskeleton [see comments]. *Science* **260,** 1124–1127.

Wang, N. and Ingber, D. E. (1994) Control of cytoskeletal mechanics by extracellular matrix, cell shape and mechanical tension. *Biophys. J.* **66,** 2181–2189.

Waring, G. O., Lynn, M. J. and McDonnell, P. J. (1994) Results of the prospective evaluation of radial keratotomy (PERK) study 10 years after surgery. *Arch. Ophthalmol.* **112,** 1298–1308.

Watsky, M. A. (1995) Keratocyte gap junctional communication in normal and wounded rabbit corneas and human corneas. *Invest. Ophthalmol. Vis. Sci.* **36,** 2568–2576.

Welch, M., Odland, G. and Clark, R. (1990) Temporal relationships of f-actin bundle formation, collagen and fibronectin matrix assembly and fibronectin receptor expression in wound contraction. *J. Cell Biol.* **110,** 133–145.

Wilson, E. E., Li, Q. and Weng, J. (1996a) The fas-gas ligand system and other modulators of apoptosis in the cornea. *Invest. Ophthalmol. Vis. Sci.* **37,** 1582–1592.

Wilson, S. E., He, Y. G. and Weng, J. *et al.* (1996b) Epithelial injury induces keratoctye apoptosis, hypothesized role for the interleukin-1 system in the modulation of corneal tissue organization and wound healing. *Exp. Eye Res.* **62,** 325–337.

Wilson, S. E., Lloyd, S. A. and He, Y. G. (1992) EGF, basic FGF and TGF beta-1 messenger RNA production in rabbit corneal epithelial cells. *Invest. Ophthalmol. Vis. Sci.* **33,** 1987–1995.

Wilson, S. E., Schultz, G. S., Chegini, N., Weng, J. and He, Y. G. (1994) Epidermal growth factor, transforming growth factor alpha, transforming growth factor beta, acidic fibroblast growth factor, basic fibroblast growth

factor and interleukin-1 proteins in the cornea. *Exp. Eye Res.* **59,** 63–71.

Wolter, J. R. (1958) Reactions of the cellular elements of the corneal stroma. *Arch. Ophthalmol.* **59,** 873–881.

Yamaguchi, T., Asbell, P. A., Ostrick, M., Safir, A., Kissling, G. E. and Kaufman, H. E. (1984) Endothelial damage in monkeys after radial keratotomy performed with a diamond knife. *Arch. Ophthalmol.* **102,** 765–769.